Mechanism of bare patch formation under *Haloxylon ammodendron* canopies and patch effects on soil microorganisms in the Gurbantunggut Desert, Northern China

Pei Liu (1105152037@qq.com)
Xinjiang University https://orcid.org/0000-0002-8860-580X
Eryang Li
Yuan Ma
https://orcid.org/0000-0003-4246-413X
Jie Lü
Qinghang Zhang

Research Article

Keywords: Haloxylon ammodendron, allelopathy, allelochemicals, Syntrichia caninervis, microbial communities

Posted Date: December 29th, 2022

DOI: https://doi.org/10.21203/rs.3.rs-2398806/v1

Abstract

Background and aims

In the Gurbantunggut Desert, *Haloxylon ammodendron* and *Syntrichia caninervis* are often found at the base of the dunes. In these areas, bare patches usually form under the *H. ammodendron* canopy, but not under other shrub canopies.

Methods

We compared the soil chemical properties under *H. ammodendron* canopy inside the bare patches (UC) and of soil under moss crust outside of *H. ammodendron* canopy bare patches (UM), and used UHPLC-MS/MS to analyze soil metabolites and metagenomic sequencing to characterize the structure of soil microflora.

Results

A total of 951 metabolites were identified in the soil samples, and 518 differential metabolites were observed. The content of amides, such as oleamide, in UC soil was significantly higher than that in UM soil, suggesting that the amides may be the main allelochemicals inhibiting *S. caninervis*. The differences in soil chemical properties and metabolites impacted soil microorganisms, but the structure and function of microbial communities did not differ significantly.

Conclusions

The amides secreted by *H. ammodendron* roots create a concentration gradient under its canopy, with high concentrations inhibiting *S. caninervis*, causing changes in soil chemical factors inside and outside the bare patch. These changes affect the abundance of microbial species and relevant metabolic pathways. The differences in microbial communities and functions are caused by a combination of soil chemical properties and metabolites, rather than a direct effect of high levels of soil metabolites such as amides.

Introduction

Plant allelopathy has been observed for more than 2,000 years. As early as 77 BC, it was found that *Juglans nigra* L. has toxic effects on neighboring plants, but it was not until the last 30 years that the researchers have systematically examined this system (Wang et al. 2016). Allelopathy is a natural phenomenon in which plants, bacteria, fungi and algae release specific metabolites into the environment during the growth process, changing the surrounding microecological environment, affecting the surrounding plants and microorganisms and resulting in mutual exclusion or promotion (Rice 1984; Olofsdotter et al. 2002; Lambers et al. 2008), and these specific metabolites are allelochemicals. Numerous studies have shown that a variety of plants can exhibit allelopathic activity on the growth of surrounding plants (Narwal 2000; Duke et al. 2000). Allelochemicals are secondary metabolites of organisms that may be secreted, volatilized or released into the environment through decomposition or leaching of plant residues. These compounds at sufficient concentration levels can affect the adjacent plant growth and community succession (Li et al. 2020b; Friedjung et al. 2013; Zhang et al. 2020; Asaduzzaman et al. 2015; Latif et al. 2017). Indeed, a variety of compounds have been isolated from various higher plants and identified as allelochemicals. These allelochemicals are generally divided into 14 categories according to their structure and composition (Rice 1984; Asaduzzaman et al. 2015). These allelochemicals can also be divided into three main categories according to the compound types: terpenes, phenols and alkaloids (Latif et al. 2017; Albuquerque et al. 2011). These identified allelochemicals play important roles in the chemical interactions of natural plant communities (Mizutani 1999).

Haloxylon ammodendron and *H. persicum* are known as exemplary psammophytic plants and are widely distributed in the Gurbantunggut Desert of Northwest China. They can physiologically adapt to harsh conditions such as high temperature, drought and sandstorms in deserts and play an important role in wind control, sand fixation, soil improvement and maintenance of biodiversity (Dong et al. 2016). These two *Haloxylon* species have nearly identical leafless green vegetative shoots, making phenotypic differentiation somewhat difficult. However, the two species have different dominant locations on the dunes, with *H. persicum* mainly growing on the tops of the dunes, while *H. ammodendron* mostly grows at the bottoms and middles of dunes in the Gurbantunggut Desert (Wu et al. 2021) In recent years, studies have found that the methanol extract of *H. persicum* contains phenolics, flavonoids, flavonols, anthocyanins, tannins, saponins and other biologically active secondary metabolites, which have allelopathic effects on *Brassica nigra* (Abdel-Farid et al. 2021). However, there is no relevant report on the allelopathic effect of *H. ammodendron* on other plants in the desert.

Terrestrial mosses are found in many biomes around the world (Glime 2006; Michel et al. 2011a), and their abundance is often affected by a complex set of factors including climate, light exposure, water availability, topography, slope, aboveground vegetation types and substrata conditions (Michel et al. 2011b). Limited by the resource availability of the Gurbantunggut Desert in Northwest China, desert mosses are scattered as biological soil crusts (Rydin 2008; Yin and Zhang 2016). In the open area of the Gurbantunggut Desert, the patch size of moss crusts, which are mainly composed of *Syntrichia caninervis* Mitt., was previously shown to be significantly influenced by soil carbon (C), nitrogen (N) and phosphorus (P) contents beneath the crusts (Li et al. 2019). Studies have shown that the presence of shrubs can cause heterogeneity of soil nutrients and moisture to form "fertile islands" in dryland areas (Li et al. 2019; Eldridge et al. 2011), so mosses can grow better under the canopy of living shrubs than in open areas (Ding and Eldridge 2021; Yin et al.

2017). However, in the sympatric community of *H. ammodendron* and *Syntrichia caninervis* along the southern margin of the Gurbantunggut Desert, bare patches are usually formed under the canopy of *H. ammodendron*, and the area outside the bare patches have rich *Syntrichia caninervis* crusts. (Hereinafter, the area under the canopy of *H. ammodendron* is also referred to as “inside the bare patch” or UC, while the area under the moss crust is also referred to as “outside the bare patch” or UM.)

Allelochemicals produced by plants can not only affect the growth and development of other plants, but also directly or indirectly affect soil microorganisms (Wang et al. 2007). Allelochemicals can be utilized or converted by soil microorganisms after entering the soil, and the metabolism of these organic compounds can in turn affect soil microbial community structures (Swenson et al. 2015) and plant root functions (Pétriacq et al. 2017). However, there are few studies on the allelopathic effect of desert plants at present, and there is no published research on whether *H. ammodendron* has allelopathic effects on *S. caninervis* under its canopy and also no published research on the impact of *H. ammodendron* secretion on the microbial community structure in bare patches. Therefore, this study examined soil metabolites using untargeted metabolomics methods (UHPLC-MS/MS technology) to study the types and differences of soil metabolites and used metagenomic sequencing to assess the structure of soil microflora inside and outside the bare patches under *H. ammodendron* canopies. Both soil metabolomics and high-throughput sequencing were conducted to elucidate whether the bare patches under the canopies are caused by allelochemicals produced by *H. ammodendron* and whether the microflora structure and function in the bare patches are affected by these allelochemicals. Thus, these results have important scientific and practical significance for desertification control in arid areas.

Materials And Methods

Study area

The Gurbantunggut Desert is located in the center of the Junggar Basin in Xinjiang, China, east of the Manas River and south of the Ulungu River (Qian et al. 2002), with coordinates spanning 44°15'–46°50'N, 84°50'–91°20'E. With an area of about 4.88×10^4 km^2, it is the second largest desert in China and the largest fixed or semi-fixed desert in China (Chen et al. 1983; Zhang et al. 1998; Zhang et al. 2010). The mean annual temperature is 7.26°C, and the average wind velocity is 11.17 m/s. The average annual precipitation is about 79.5 mm, mostly in the spring, and the average annual evaporation is 2,606 mm. Because the Gurbantunggut Desert has a relatively evenly distributed precipitation season, with a certain amount of rain and snow in spring and winter, the vegetation is relatively dense and covered with more than 200 species of vegetation. The vegetation is dominated by *H. ammodendron* and *H. persicum*, accompanied by herbaceous plants and many short-lived plants, such as *Ceratocarpus arenarius*, *Ephedra distachya*, *Artemisia wellbyi* and *Petrosimonia sibirica*. Part of the desert surface is covered with biological soil crusts (Zhang et al. 2022), among which, the moss crusts are mainly dominated by *Tortula* and related moss, such as *S. caninervis* (Li et al. 2019; Ji et al. 2013).

Sample collection

In September 2021, six soil samples were collected inside and outside of three different bare patches (Fig. 1) at a depth of 0–4 cm in the sympatric area of *H. ammodendron* and *S. caninervis* with an obvious bare patch, and the surface of the sampling plots with plant litters and other impurities were cleaned. The soil inside the bare patches showed obvious agglutination, and the soil outside the bare patches under the moss crusts showed no such phenomenon. Samples were packed into sterilized self-sealing bags that were placed in iceboxes and brought back to the laboratory promptly. After grinding, the samples were subjected to chemical property determination, metabolomic determination and metagenomic sequencing.

Methods

Soil chemical properties inside and outside the bare patches

The soil samples were air-dried in the laboratory and passed through 60-mesh sieves to remove plant residues and fine roots, and 10-g soil samples were weighed to determine the pH value. The remaining soil samples were ground and passed through 2-mm sieves for the determination of soil organic carbon (SOC), total phosphorus (TP), total potassium (TK), total nitrogen (TN), ammonium nitrogen (NH_4^+-N), nitrate nitrogen (NO_3^--N), soil microbial biomass carbon (MBC), microbial biomass nitrogen (MBN) and total salts (TS) as well as eight major ions (K^+, Ca^{2+}, Na^+, Mg^{2+}, Cl^-, SO_4^{2-}, CO_3^{2-}, HCO_3^-).

Determination of SOC was conducted using the dichromate oxidation method (Jones and Willett 2006). The TN concentration was determined using the Kjeldahl method. NH_4^+-N and NO_3^--N were extracted with potassium chloride (KCl) solution and measured using spectrophotometry (Kachurina et al. 2000). The TP content was measured using the molybdenum-antimony colorimetric method after extraction with Na_2CO_3. TK was dissolved by NaOH and quantified using the flame photometric method. MBC and MBN were measured using the chloroform fumigation extraction (FE) method. The pH value was determined using a pH meter. K^+, Ca^{2+}, Na^+, Mg^{2+}, Cl^- and SO_4^{2-} were detected using ion chromatography. CO_3^{2-} and HCO_3^- were detected using potentiometric titration, and TS was detected using the weight method (Bao 2000).

Metabolite extraction and LC-MS analysis

One-hundred-milligram soil samples were individually ground with liquid nitrogen, and the homogenates were placed in Eppendorf (EP) tubes, and after 500 µL of prechilled 80% methanol was added to each EP tube, homogenates were vortexed. The EP tubes were incubated on ice for 5 min and then centrifuged at 15,000 × *g* and 4°C for 20 min. LC-MS-grade water was added to a certain amount of supernatant and diluted to a methanol content of 53%.

Samples were centrifuged again at 15,000 × *g* and 4°C, and the supernatant was collected after centrifugation for 20 min for LC-MS detection and analysis (Want et al. 2013).

UHPLC-MS/MS analyzes were performed using a Vanquish UHPLC system (Thermo Fisher, Dreieich, Germany) coupled with an Orbitrap Q Exactive™ HF mass spectrometer (Thermo Fisher) by Novogene Co., Ltd. (Beijing, China). Samples were injected into a Hypesil GOLD column (100 × 2.1 mm, 1.9 μm) at a flow rate of 0.2 mL/min using a 17-min linear gradient. The eluents for the positive polarity mode were eluent A (0.1% formic acid in water) and eluent B (methanol). Eluent A (5 mM ammonium acetate, pH 9.0) and eluent B (methanol) were used in negative polarity mode. The solvent gradient was set as follows: 98% A and 2% B, 1.5 min; 98–0% A and 2–85% B, 3 min; 0% A and 100% B, 10 min; 0–98% A and 100–2% B, 10.1 min; 98% A and 2% B, 12 min. The scanning range of mass spectrometry was m/z 100–1,500. The settings of the ESI source were as follows: spray voltage, 3.5 kV; sheath gas flow rate, 35 psi; auxiliary gas flow rate, 10 L/min; capillary temperature, 320°C; iontophoresis RF level (S-lens RF level), 60; auxiliary gas heater temperature, 350°C; polarity, positive/negative; MS/MS secondary scans, data dependent.

The raw data files generated by UHPLC-MS/MS were processed using Compound Discoverer 3.1 (CD 3.1, Thermo Fisher), and screening for retention time, mass-to-charge ratio and other parameters were performed for peak alignment, peak picking and quantitation of each metabolite. Actual mass tolerance (5 ppm) and retention time tolerance (0.2 min) were set for peak alignment of different samples to make identification more accurate. Peak extraction was performed with the following settings: signal-to-noise ratio, 3:1; signal intensity tolerance, 30%; actual mass tolerance, 5 ppm. Minimum signal intensity and other information were set, while the peak areas were quantified. After that, peak intensities were normalized to the total spectral intensity. The normalized data were used for molecular formula prediction, which is based on molecular ion peaks, fragment ions and additive ions. Bare samples were used to remove background ions, and peaks were then matched with the mzCloud (https://www.mzcloud.org/), mzVault and MassList databases to obtain metabolite qualitative and relative quantitative results. When the data were not normally distributed, the area normalization method was used to normalize data. The identified metabolites from the soil metabolome were annotated using the Kyoto Encyclopedia of Genes and Genomes (KEGG) database, the Human Metabolome Database (HMDB) (https://hmdb.ca/metabolites) and the LIPIDMaps database (http://www.lipidmaps.org/).

DNA extraction and high-throughput sequencing

Genomic DNA were extracted from soil samples using the FastDNA® SPIN Kit for soil (MP Biomedicals, Solon, OH, USA), and the operation steps were carried out according to the kit instructions. The length and integrity of the genomic DNA were assessed by agarose gel electrophoresis, and the concentration and purity of DNA were detected using a NanoDrop2000 instrument (Thermo Fisher Scientific, Waltham, MA, USA). After confirming the integrity and concentration of genomic DNA met the sequencing requirements, Novogene Co., Ltd. (Beijing, China) was commissioned to conduct metagenomic sequencing. DNA samples were randomly fragmented by sonication (Covaris, Woburn, MA, USA), and then, the DNA fragments were end-polished, A-tailed and ligated with the full-length adaptor for Illumina sequencing with further PCR amplification. At last, PCR products were purified using the AMPure XP system (Beckman Coulter, Indianapolis, IN, USA), and libraries were analyzed for their size distribution by the Agilent 2100 Bioanalyzer (Agilent, Santa Clara, CA, USA) and quantified using real-time PCR. After library construction, the library preparations of soil samples inside and outside the bare patches were sequenced on an Illumina NovaSeq 6000 platform (Illumina, San Diego, CA, USA).

For the raw data obtained from metagenomic sequencing, quality control and adaptor removal were performed using trimmomatic (v0.39) (Bolger et al. 2014). MultiQC (v1.7) (Ewels et al. 2016) software was used for multiple quality control processes and summarization of analysis results. Taxonomic annotation was performed based on reads using kraken2 (v2.0.8-beta) (Wood and Salzberg 2014). Clean reads were assembled using MEGAHIT (v1.1.3) (Li et al. 2015), and contigs with a length over 300 bp were selected as the final assembly result. Then, the contigs were used for further gene prediction and annotation by Prokka (v1.13.3) (Seemann 2014). All predicted genes with the criteria of identity > 95% and overlap > 90% were clustered using CD-HIT (v4.8.1) (Fu et al. 2012), and the longest sequences from each cluster were selected as representative sequences to construct a non-redundant gene catalog. Reads after quality control were mapped to the representative sequences using Salmon (v0.14.0) (Patro et al. 2017), and gene abundances in each sample were evaluated. The amino acid sequences of representative sequences were made on the basis of KofamKOALA (Aramaki et al. 2019) alignment against the KEGG database (https://www.genome.jp/kegg/pathway.html) and were annotated with the CAZy Database (https://www.cazy.org) (Lombard et al. 2013) using Diamond (v0.8.22).

Statistical analysis

All data were processed using Excel and expressed as the mean ± standard deviation (S.D.). Differences between UC and UM were determined by *t*-test at a $P < 0.05$ significance level. The metabolomic data were logarithmically transformed and normalized using metaX (Wen et al. 2017), and partial least squares discriminant analysis (PLS-DA) was performed to obtain the variable importance in the projection (VIP) value of each metabolite. The statistical significance of each metabolite between the UC and UM groups was calculated based on the *t*-test as implemented in R (v.4.1.2), and the fold change (FC) of each metabolite between the two groups was calculated. Finally, metabolites with $P < 0.05$, VIP > 1, and either FC ≥ 1.5 or FC ≤ 0.667 were identified as differential metabolites. The soil chemical properties, differential metabolites, microbial and functional diversity of the two groups (i.e., UC and UM) were determined using R packages and displayed using ggplot2 package in R 4.1.2. Linear discriminant analysis (LDA) effect size (LEfSe) for Cyanobacteria and Chlorophyta was also conducted using LEfSe software. Sunburst charts were created in Excel 2021 (Microsoft Corp., Redmond, WA, USA). Clustering bubble charts were also plotted using R software.

Results

Analysis and comparison of soil chemical properties inside and outside the bare patches under *Haloxylon ammodendron* canopies

The soil chemical properties inside the bare patches under the canopies of *H. ammodendron* and outside the bare patches under the crusts of *S. caninervis* (i.e., UC and UM) are shown in Fig. 2 (and Online Resource 1,2). The contents of K^+, Ca^{2+}, Na^+, Mg^{2+}, Cl^-, SO_4^{2-}, CO_3^{2-}, HCO_3^- and total salt (TS) in soil inside the bare patches were higher than those outside the patches, and there were significant differences in the contents of CO_3^{2-}, HCO_3^- and TS ($P < 0.05$; Fig. 2a). In addition, there were no significant differences in soil TK, SOC, NH_4^+-N, MBC and MBN between inside and outside the bare patches. The contents of TP and NO_3^--N in soil inside the bare patches were significantly higher than those outside the bare patches under moss crusts, among which the NO_3^--N contents were 21.665 mg/kg and 8.776 mg/kg, respectively, and the difference was highly significant ($P < 0.01$). The soil both inside the bare patches and under the moss crusts was alkaline, and the soil pH under the canopy was 10.01, which was significantly higher than that under the moss, which was 8.73 ($P < 0.01$). However, the soil TN content under the moss was significantly lower than that in soil inside the bare patches ($P < 0.01$; Fig. 2b).

Soil metabolite identification and bioinformatic analysis

Soil metabolite identification and annotation

In this study, LC-MS was used for untargeted metabolite profiling of soils inside and outside the bare patches. A total of 951 metabolites were identified in soil samples, of which 615 and 336 were identified in positive and negative ion mode, respectively. Metabolites in soil samples were annotated using three different databases. A total of 610 metabolites were annotated using the KEGG database, including 297 and 313 in positive and negative ion mode, respectively. In HMDB, 446 metabolites were identified in the data, including 273 and 173 in positive and negative ion mode, respectively. Soil sample metabolites were also annotated using the LIPID MAPS Database, with a total of 163 annotated metabolites (79 and 84 in positive and negative ion mode, respectively).

Differential metabolite analysis

Principal component analysis of 951 metabolites in soils inside and outside the bare patches showed that the first principal component (PC1) and the second principal component (PC2) explained 51.41% and 13.52% of the variability, respectively (Fig. 3a). The identified samples in soils inside (UC) and outside (UM) the bare patches were clearly separated along the first axis, indicating that the metabolite compositions of the two samples were quite distinct. The six replicate samples inside the bare patches were distributed in the left side of the plot, and the six biological replicates outside the bare patches were concentrated in the right side of the plot, also showing a clear separation between UC and UM soil. Taken together, PCA showed that there were significantly different metabolic profiles between soils inside the bare patches under the canopy of *H. ammodendron* and outside the bare patches under the crusts of *S. caninervis.* After application of VIP ≥ 1, $P < 0.05$ and either FC > 1.5 or FC < 0.667 thresholds, $\log_2$(FC) values were used to construct a volcano map (Fig. 3b), which provides a visual representation of the overall distribution of metabolite differences between inside and outside of the patches.

High relative abundance differential metabolite analysis

Among the 951 metabolites detected by metabolomic analysis, a total of 518 significantly different metabolites were screened, of which 230 were up-regulated and 288 were down-regulated. The identified 518 differential metabolites were among nine types of compounds, and the classification results are summarized in Fig. 4a. Among these metabolites, lipids and lipid-like molecules were the most numerous differential metabolites, and organoheterocyclic compounds were scattered among more categories. There were 64 differential metabolites among benzenoids. Among the 27 differential metabolites of phenylpropanoids and polyketides, 2 were coumarins and their derivatives, 8 were flavonoids, and 6 were cinnamic acids and their derivatives. Among the nine classes of compounds, lipids and lipid-like molecules accounted for the largest proportion of differential metabolites, and fatty acyls comprised the most differential metabolites; prenol lipids (including terpenoids) included 20 identified differential metabolites.

Among the 518 differential metabolites, the top 30 with the highest abundance were selected for further analysis, and their relative quantification values were normalized; a bubble chart of the top 30 different metabolites is shown in Fig. 4b. Among the top 30 different metabolites, the relative abundance of oleamide((Z)-9-octadecenamide) (58.02%) was highest in UC soil, followed by oleoyl ethylamide (9.43%), hexadecanamide (7.83%), melibiose (4.75%), d-(+)-maltose (4.71%) and stearamide (3.65%). In contrast, the top six metabolites in relative abundance in UM soil were melibiose (21.92%), d-(+)-maltose (20.46%), oleamide (13.75%), α,α-trehalose (8.06%), xanthurenic acid (3.27%) and 7-methoxyflavone (2.65%). The relative abundance of oleamide was elevated in both UC and UM, but the relative content in UC was 7.13 times higher than that in UM. Therefore, it is speculated that several aliphatic compounds, such as oleamide, may have an important relationship with the formation of the bare patches.

Analysis of allelochemicals in soil metabolites

By searching the relevant literature and metabolite databases, among the 518 differential metabolites, we also found some metabolites whose relative abundance were not very high, but had been reported as relatively clear allelochemicals with allelopathic effects. These differential metabolites were selected and classified as 14 allelochemicals (Rice 1984; Asaduzzaman et al. 2015) to obtain Table 1. Compared to UM soil, all cinnamic acids and their derivatives were up-regulated in UC soil; among the simple phenols, benzoic acid and their derivatives, only salicylic acid was down-regulated, while the remaining nine were up-regulated. There was only one type of anthraquinone, which was up-regulated. Two long-chain fatty acids were both up-regulated. There were two types of coumarins and their derivatives; one was up-regulated, and the other was down-regulated. Four terpenoids were up-regulated, and five were down-regulated. Among the flavonoids, only quercetin and hesperidin were up-regulated, while the remaining five were down-regulated. The results suggested that cinnamic acid and its derivatives and benzoic acid and its derivatives may have some effect on the formation of the bare patches.

Table 1
Differential plant metabolites analysis results of soils inside and outside the bare patches

Serial number	Compound classification	Compound name	Formula	FC	VIP	*P* value	up & down	Average relative abundance	
								inside	outside
1	**Simple phenols, benzoic acid and derivatives**	Syringic acid	$C_9H_{10}O_5$	4.202806157	1.1838	1.60E-05	up	0.000153406	6.17183E-05
		2,6-Dihydroxybenzoic acid	$C_7H_6O_4$	4.233184905	1.1281	0.001180321	up	0.000127209	5.08117E-05
		Benzoic acid	$C_7H_6O_2$	2.764976581	1.1459	8.25E-05	up	0.000106209	0.003062116
		2,4-Dihydroxybenzoic acid	$C_7H_6O_4$	6.26482979	1.2367	5.96E-05	up	9.27698E-05	2.50386E-05
		5-Methoxysalicylic acid	$C_8H_8O_4$	3.488120103	1.1960	0.000214158	up	9.02394E-05	4.37438E-05
		Salicylic acid	$C_7H_6O_3$	0.19891281	1.0111	0.009215969	down	9.02394E-05	4.37438E-05
		4-Hydroxy-3-methylbenzoic acid	$C_8H_8O_3$	2.181165291	1.1241	0.000380836	up	4.53118E-05	3.51265E-05
		Anthranilic acid	$C_7H_7NO_2$	1.795753083	1.2109	3.06E-05	up	4.52291E-05	4.25876E-05
		2-Anisic acid	$C_8H_8O_3$	1.670227843	1.1358	0.000438552	up	3.56382E-05	3.60788E-05
		Vanillin	$C_8H_8O_3$	2.102471299	1.1223	0.000189862	up	3.34014E-05	2.68625E-05
2	**Benzoquinones, anthraquinones and complex quinones**	Dantron	$C_{14}H_8O_4$	4.287783164	1.2690	3.60E-10	up	5.94393E-05	2.34397E-05
3	**Coumarins and derivatives**	8-(1,2-dihydroxy-3-methylbut-3-en-1-yl)-7-methoxy-2H-chromen-2-one	$C_{15}H_{16}O_5$	0.437695406	1.1965	0.000224964	down	0.000117545	0.000454091
		Scopoletin	$C_{10}H_8O_4$	2.50381503	1.2667	2.25E-09	up	5.60033E-05	3.78202E-05
4	**Cinnamic acid and derivatives**	Chlorogenic acid	$C_{16}H_{18}O_9$	3.987573296	1.2519	3.53E-08	up	0.000194449	8.24534E-05
		Sinapinic acid	$C_{11}H_{12}O_5$	3.43540246	1.2617	3.72E-09	up	8.46551E-05	4.16665E-05
		Caffeic acid	$C_9H_8O_4$	2.557980522	1.2511	2.35E-07	up	7.57151E-05	5.00492E-05
		Ferulic acid	$C_{10}H_{10}O_4$	2.444441722	1.1386	0.000715194	up	5.09861E-05	3.52683E-05
		4-Methoxycinnamic Acid	$C_{10}H_{10}O_3$	1.993068117	1.2073	4.02E-05	up	4.66041E-05	3.95379E-05
5	**Flavonoids**	6-Hydroxyflavone	$C_{15}H_{10}O_3$	0.441388755	1.1910	0.000958965	down	0.000382122	0.001463839
		7-hydroxy-3-(4-methoxyphenyl)-4H-chromen-4-one	$C_{16}H_{12}O_4$	0.400514769	1.3009	1.68E-05	down	0.00036694	0.001549134
		Biochanin A	$C_{16}H_{12}O_5$	0.458223694	1.2500	6.37E-05	down	0.000100567	0.000371101

Serial number	Compound classification	Compound name	Formula	FC	VIP	*P* value	up & down	Average relative abundance	
								inside	outside
		Hesperetin	$C_{16}H_{14}O_6$	2.478566699	1.2210	3.99E-06	up	8.24081E-05	5.62187E-05
		Formononetin	$C_{16}H_{12}O_4$	0.547408683	1.0676	0.001678057	down	7.5867E-05	0.000234344
		Isorhamnetin	$C_{16}H_{12}O_7$	0.179122504	1.3185	2.33E-06	down	1.82167E-05	0.000171962
		Quercetin	$C_{15}H_{10}O_7$	2.320284484	1.0952	0.00170448	up	1.1208E-05	8.16769E-06
6	**Long-chain fatty acids**	Palmitic acid	$C_{16}H_{32}O_2$	10.1920176	3.45E-06	1.233171672	up	0.000706992	0.000117291
		Erucic acid	$C_{22}H_{42}O_2$	6.952048227	1.3477	2.74E-08	up	0.000203171	4.94152E-05
7	**Terpenoids**	T-2 Triol	$C_{20}H_{30}O_7$	0.526193412	1.0640	0.003492624	down	0.000832709	0.002675839
		Diacetoxyscirpenol	$C_{19}H_{26}O_7$	0.550650178	1.1059	0.002326473	down	0.000478417	0.00146907
		Farnesyl pyrophosphate	$C_{15}H_{28}O_7P_2$	2.974688685	1.1846	3.34E-05	up	0.000334549	0.000190165
		p-Mentha-1,3,8-triene	$C_{10}H_{14}$	3.710304839	1.3089	8.47E-05	up	0.000232129	0.000105787
		Oleanolic acid	$C_{30}H_{48}O_3$	9.661888842	1.3336	8.70E-06	up	0.000119701	2.09483E-05
		Perillartine	$C_{10}H_{15}NO$	0.476463271	1.1140	0.002142543	down	9.29555E-05	0.000329881
		(+)-ar-Turmerone	$C_{15}H_{20}O$	0.271876302	1.1275	0.002308152	down	2.271E-05	0.00014124
		Obacunone	$C_{26}H_{30}O_7$	0.261503105	1.1815	0.000982246	down	1.33427E-05	8.62738E-05
		Betulin	$C_{30}H_{50}O_2$	2.901615726	1.2566	7.59E-05	up	8.18891E-06	4.77197E-06
8	**Purines and nucleosides**	Adenosine	$C_{10}H_{13}N_5O_4$	0.283971902	1.2973	3.20E-05	down	0.003995551	0.023791028
		Kinetin	$C_{10}H_9N_5O$	0.269923109	1.2911	7.01E-06	down	4.3796E-05	0.000274351
		Guanosine	$C_{10}H_{13}N_5O_5$	0.302366869	1.1263	0.000289946	down	3.15629E-05	0.000176504
		1-Methylguanosine	$C_{11}H_{15}N_5O_5$	1.671121979	1.0010	0.018022588	up	2.15638E-05	2.18187E-05
		1-Methyladenosine	$C_{11}H_{15}N_5O_4$	0.24641588	1.3065	3.55E-05	down	4.00013E-06	2.74484E-05
9	**Amino acids and polypeptides**	L-Phenylalanine	$C_9H_{11}NO_2$	0.126325562	1.3378	4.70E-08	down	0.000194425	0.002602398
		DL-o-Tyrosine	$C_9H_{11}NO_3$	0.651884545	1.1168	0.00342416	down	0.000104111	0.000270047
		L-Tyrosine	$C_9H_{11}NO_3$	2.530345373	1.2155	2.84E-06	up	5.3795E-05	3.59479E-05

Serial number	Compound classification	Compound name	Formula	FC	VIP	*P* value	up & down	Average relative abundance	
								inside	outside
		Ecgonine methyl ester	$C_{10}H_{17}NO_3$	0.187535671	1.2696	4.98E-05	down	3.62863E-05	0.000327168
		N-Acetyl-L-tyrosine	$C_{11}H_{13}NO_4$	5.762366196	1.0110	0.002282007	up	2.14701E-05	6.30005E-06
		2-Hydroxyphenylalanine	$C_9H_11NO_3$	0.051583714	1.3240	2.78E-07	down	1.28119E-05	0.000419966

KEGG enrichment analysis

Pathway enrichment analysis was assessed using the hypergeometric test to elucidate the specific changes in soil metabolic processes, and there were 99 and 108 metabolic pathways enriched in the positive and negative ion mode, respectively. According to the *p*-value of all metabolic pathways, the top 10 metabolic pathways are shown in Fig. 5, and of these, only phenylalanine metabolism significantly differed between inside and outside bare patches. Moreover, phenylalanine metabolism is closely associated with phenylalanine, tyrosine and tryptophan biosynthesis and phenylpropanoid biosynthesis among the top 10 metabolic pathways. Phenylalanine, tyrosine and tryptophan biosynthesis are associated with phenylalanine metabolism and phenylpropanoid biosynthesis via l-tyrosine, which is the upstream metabolic pathway of the other two metabolic pathways. Chlorogenic acid, caffeic acid, ferulic acid, l-tyrosine and scopoletin were enriched within the phenylpropanoid biosynthesis pathway, and all of these compounds were identified as allelochemicals (Table 1) and were concentrated in UC soil at significantly higher levels than in UM soil.

Soil microbial diversity and community structure inside and outside the bare patches

Analysis of microbial composition of soils inside and outside the bare patches

The quality control data of metagenomic sequencing was annotated using the Kraken2 standard library. The annotation results included archaea, bacteria, fungi and viruses (Online Resource 3). The microbial communities inside and outside the bare patches under the canopy of *H. ammodendron* in the southern margin of the Gurbantunggut Desert were dominated by bacteria, and the average abundance of bacterial sequences among all microbial sequences in soils both inside and outside the bare patches was over 97%. All species were normalized with vegan package and imported into the microeco package for analysis. A total of 1106 species of archaea belonging to 157 genera, 49 families, 31 orders, 17 classes and 15 phyla were identified, while 17,741 species of bacteria belonging to 2237 genera, 517 families, 215 orders, 88 classes and 84 phyla were identified. Additionally, 3417 species of fungi belonging to 1389 genera, 484 families, 171 orders, 53 classes and 8 phyla were identified.

Diversity analysis of soils inside and outside the bare patches

The alpha diversity of microorganisms in soils inside and outside the bare patches under the canopy of *H. ammodendron* is shown in Fig. 6a. The observed species and chao1 diversity indexes were significantly lower in UC soil than in UM soil, that is, the number of species in UM soil was significantly higher than that in UC soil ($P < 0.05$). The Simpson diversity index of UC soil was higher than that of UM soil, but not significantly ($P > 0.05$), indicating a more homogeneous microbial community structure in UC soil compared to UM soil.

The soil microbial species relative abundance in UC and UM soil was analyzed by principal co-ordinate analysis (PCoA) based on Bray–Curtis distance (Fig. 6b). The variance of the first two principal coordinates accounted for 88.0% of the total variance. The microbial communities of the UC and UM groups were clustered separately and separated along the principal coordinate axis, but there was no significant difference in the microbial community structure between UC and UM.

Comparison of microbial communities in soils inside and outside the bare patches

The top 10 phylum based on microbial abundance in UC and UM soil were Actinobacteria, Proteobacteria, Planctomycetes, Bacteroidetes, Cyanobacteria, Firmicutes, Ascomycota, Gemmatimonadetes, Euryarchaeota and Deinococcus-Thermus (Fig. 7a). Among them, Actinobacteria and Proteobacteria were most abundant in UC and UM soils. The relative abundance of Actinobacteria in UC soil was 58.47%, which was significantly higher than 55.18% in UM soil ($P < 0.05$). The relative abundance of Proteobacteria in UC soil was 28.98%, which was significantly lower than 33.67% in UM soil. The relative abundances of other phyla, such as Gemmatimonadetes, Euryarchaeota, and Deinococcus-Thermus, were all less than 1%. The relative abundance of Gemmatimonadetes and Deinococcus-Thermus was significantly higher in UC soil than in UM soil.

In addition, the top 30 genera among the annotated microbial species were selected for cluster heatmapping (Fig. 7b), which shows the top 30 species are all Bacteria, of which 21 genera belong to Actinobacteria, 8 genera belong to Proteobacteria and 1 genus belongs to Cyanobacteria. Among the Actinobacteria, seven genera, *Rhodococcus*, *Corynebacterium*, *Microbacterium*, *Mycobacterium*, *Mycolicibacterium*, *Streptomyces* and *Cellulomonas*, had significantly higher relative abundance in UC soil than UM soil ($P < 0.05$). The relative abundance of six genera, *Pseudonocardia*, *Geodermatophilus*, *Blastococcus*, *Microvirga*, *Bradyrhizobium* and *Methylobacterium* in UC soil was significantly ($P < 0.05$) lower than that in UM soil, with *Microvirga* and *Methylobacterium* showing a highly significant difference ($P < 0.01$). The cluster heatmap also showed significant differences between the dominant genera in UC and UM soil, suggesting that the formation of bare patches did have an impact on the soil microbial community.

Linear discriminant analysis (LDA) effect size (LEfSe), with an LDA threshold of 3.5, was used to identify taxa of Cyanobacteria and Chlorophyta that differed between inside and outside the bare patches (Fig. 7c,d). In UC soil, the differential taxa of Cyanobacteria that were significantly enriched at the genus level were *Microcoleus* and *Oscillatoria*, both of which belong to Oscillatoriales. The genera significantly enriched in UM soil were *Nostoc*, *Scytonema*, *Calothrix* and *Allocoleopsis*, with *Nostoc*, *Scytonema* and *Calothrix* all belonging to Nostocales, and *Allocoleopsis* belonging to Oscillatoriales. Cluster heatmap analysis of the top 30 genera of Cyanobacteria in terms of relative abundance (Fig. 7e) showed that there were no significant differences ($P > 0.05$) in the biomarker genera identified by LEfSe (*Microcoleus*, *Oscillatoria*, *Nostoc*, *Scytonema*, *Calothrix* and *Allocoleopsis*) in soils inside and outside the bare patches. Among the top 30 genera with the highest abundance, *Synechococcus* and *Cyanobium*, both belonging to Synechococcales, were significantly higher in UC soil than in UM soil. Chen et al. found that microorganisms of Synechococcales were highly adapted to alkalinity, growing normally at conditions of pH up to 10 or even higher (Chen 2013). As soil pH within the bare patches (10.013) was significantly higher than UM (8.737), we speculate that Synechococcus may have a dependence on highly alkaline environments.

The differential taxa of Chlorophyta that were significantly enriched at the genus level in UC soil were *Monoraphidium* and *Coccomyxa*, while the only genus that was significantly enriched in UM soil was *Trebouxia*. The top 30 genera with the highest abundance among Chlorophyta were also subjected to cluster heatmapping (Fig. 7f), which revealed no significant differences ($P > 0.05$) in the biomarker genera selected by LEfSe (*Monoraphidium, Coccomyxa* and *Trebouxia*; Fig. 7d) in UC and UM soil. Among Chlorophyta, the genera *Chlamydomonas*, *Micromonas*, *Monoraphidium*, *Chlorella*, *Coccomyxa*, *Volvox*, *Dunaliella*, *Auxenochlorella*, *Ostreococcus* and *Chloropicon* all had relative abundances above 1% both inside and outside the pare patches, but only *Auxenochlorella* and *Chloropicon* were significantly different between UC and UM soil, suggesting that the secretions of *H. ammodendron* had no significant effect on the Chlorophyta community.

Functional diversity of microbial communities in soils inside and outside the bare patches

Based on the relative abundance of KEGG ortholog groups (Kos) and CAZy families, PCoA was performed according to Bray–Curtis distance (Fig. 8a,b), and the types of soil microbial KOs and CAZy families and their relative abundance inside and outside the bare patches were not significantly associated with metabolites of *H. ammodendron* or the formation of bare patches. Eight KEGG metabolic pathways with relative abundance of more than 1% significantly differed between UC and UM soil, namely Starch and sucrose metabolism (ko00500); Secretion system (ko02044); Purine metabolism (ko00230); Protein kinases (ko01001); Peptidoglycan biosynthesis and degradation proteins (ko01011); Peptidases and inhibitors (ko01002); Glycine, serine and threonine metabolism (ko00260) and Chromosome and associated proteins (ko03036). Six of these metabolic pathways were significantly more abundant in the bare patches than in soil under the moss crusts (Fig. 8c). CAZy database annotation analysis showed that there were eight CAZy families with relative abundance over 1% that were significantly different, and they belonged to four CAZy families; of the eight families GT9, GH18, GH16, GH0, CE14, CBM50, CBM5 and CBM13, the relative abundance of GH18, CBM50, CBM5 and CBM13 was significantly higher in UC soil than that in UM soil (Fig. 8d).

Relationships of microbial community with soil variables

Seven soil chemical indicators that were significantly different between UC and UM soil (Table 1, Online Resource 1) and the top eight metabolites with an average relative abundance above 0.1% in the soil metabolome and significantly higher content in UC soil than in UM soil were selected as soil variables to analyze the relationship with microbial communities (Table 1 and Fig. 4).

The results of Mantel test analysis showed that there was highly significant correlation ($P < 0.01$) between archaeal community structure and NO_3^--N, and the bacterial community structure was only significant correlated with TN. The microbial community structure was mainly influenced by these two soil chemical properties, while fungal communities were not significantly correlated with any of these soil variables (Fig. 9a). The correlation analysis between the significantly different soil variables showed that there were significant positive correlations between almost all of the selected soil variables except TN, which was strongly negatively correlated with almost all of the other soil variables. The correlation heatmap analysis showed that among the top 10 most abundant phyla, the relative abundance of three phyla, Actinobacteria, Gemmatimonadetes and Deinococcus-Thermus, were significantly positively correlated with some of the soil variables; additionally, Proteobacteria abundance was significantly negatively correlated with some of the soil variables, and abundances of the other six phyla were not significantly correlated with the soil variables (Fig. 9b).

Discussion

Various types of biocrusts are fully developed on the southern margin of the Gurbantunggut Desert, with a continuous distribution and covering a large area (Zhang et al. 2005). Among them, moss crusts, mainly composed of *Syntrichia caninervis*, are usually found in the lowlands between sand dunes and develop particularly prominently under low scrub species such as *Ephedra distachya* (Ji et al. 2013; Wang et al. 2006; Zhang et al. 2004) and *Kalidium foliatum* (Wang et al. 2021). Yin et al. (Yin et al. 2017) found the same phenomenon, with moss crusts widely distributed in open areas and under desert shrubs, and observed that mosses under living shrub canopies grew better than those in open areas. The under-canopy of the small shrub-like tree *H. ammodendron* should be favorable for the growth of moss crusts. However, in areas where the *H. ammodendron* and mosses are sympatric, bare patches form under the canopy of *H. ammodendron*, and *S. caninervis* does not survive under its canopy. In contrast, outside the bare patches there is profuse growth of *S. caninervis*. Accordingly, we are interested in knowing what causes the bare patches under the canopy of *H. ammodendron*. Moreover, soil microorganisms are very sensitive to environmental changes and, as an important indicator of soil environmental quality (Zak et al. 1994) microbial diversity can reflect soil environmental conditions to some extent (Sun et al. 2010). Changes in the soil environment and nutrient cycling can lead to differences in soil microbial communities (Zak et al. 2003; Johnson et al. 2004; Bird et al. 2011). Accordingly, we were also interested in whether the formation of bare patches under the canopy of *H. ammodendron* also alters the microbial community and function.

In this study, we explored the mechanism of the formation of bare patches under the canopy of *H. ammodendron* in the southern margin of the Gurbantunggut Desert by using soil metabolomic data to study the differential metabolites inside and outside the bare patches. At the same time, metagenomic sequencing was used to study the community structure and function of soil microorganisms inside and outside the bare patches, while potential effects of metabolites of *H. ammodendron* on the soil microorganisms under its canopy were also examined by identifying differential metabolites.

Relationship between bare patch and soil chemical properties

Saline soils in the arid and semi-arid regions of northwest China are mostly dominated by water-soluble chloride and sulphate, and salt ions have an effect on plant growth, with excess salt inhibiting plant growth (Liu 2010). There were significant differences in CO_3^{2-}, HCO_3^- and TS contents, but not in Na^+, Cl^- and SO_4^{2-} contents, between UC and UM soil. Gene Ontology annotation of whole genome sequencing of *S. caninervis* showed that its genome contains genes related to the response to salt stress (GO:0009651) (Silva et al. 2021). As well, Liu et al. (Liu et al. 2016) used different concentrations of NaCl solution in treatments of *S. caninervis*. Their results showed that at a concentration of 100 mmol NaCl, the cell structure of *S. caninervis* leaves remained intact, the chloroplast stroma was homogeneous, and the ultrastructure of the mesophyll cells only showed minor changes, which basically had no effect on its normal growth. These present analysis concluded that the concentration of soil TS in UC was not the main cause of bare patch formation.

Relationship between bare patch formation and soil metabolites

Soil metabolites are derived from plant root secretions, soil microbes and decomposition products of soil organic matter by plants and microorganisms (Cheng et al. 2018). However, the distinction between metabolites of plants or microbial metabolites remains the greatest challenge in soilomics (White et al. 2017). In the present study, the untargeted soil metabolomics results showed that the relative abundance of oleamide (58.02%) was highest in UC soil. In contrast, oleamide was still higher and among the top six metabolites in terms of relative abundance in UM soil. The relative abundance of oleamide was comparatively higher in both UC and UM soil, and the content was significantly higher in UC soil than in UM soil, with the relative content of UC being 7.13 times higher than that of UM soil, suggesting an important role for oleamide in the formation of the bare patches under the canopy of *H. ammodendron*.

Studies on the allelopathy of amide compounds such as oleamide are less common, but some relevant findings have been reported. Shao et al. (Shao et al. 2016) found that oleamide can inhibit the growth of the cyanobacterium *Microcystis aeruginosa* by damaging its electron accepting side of photosystem II, as well as by destroying fatty acid constituents, distorting the thylakoid membrane, and causing loss of cell membrane integrity. Oleamide was also identified in a study by Dong et al. (Dong et al. 2018) to have an allelopathic effect in an aqueous extract of *Typha orientalis* on *Microcystis aeruginosa*. Previous researchers have also inferred that the oleamide in *Pistia stratiotes* should have a strong inhibitory effect on algal activity, based on stearamide isolated from the extract of *Pistia stratiotes* functioning as a allelochemical with algae inhibitory activity (Wu et al. 2016). The results of these studies suggest that oleamide may be allelopathic to some prokaryotes. Xiao et al. (Xiao et al. 2015) also found the presence of oleamide in a study of allelopathy in the rhizosphere soil of *Polygonatum odoratum*, which may be associated with the difficulties in continuous cropping of *P. odoratum*, and surmised that the amide compounds may act as allelochemicals. In the present study, the relative contents of three amide compounds in UC soil, oleoyl ethylamide (9.43%), hexadecanamide (7.83%) and stearamide (3.65%), were all significantly higher than that in UM soil. In a study of tobacco root exudates, Yu et al. (Yu et al. 2013) identified hexadecanamide, oleamide and stearamide, and inferred that amide compounds may be allelochemicals in two different tobacco root exudates. It has already been reported that oleamide is contained in the secretion of *H. ammodendron* roots (Zhang et al. 2006; 2007), and it can be reasonably inferred that the oleamide present in soil inside the bare patch originates from *H. ammodendron*. In this study, the relative content of oleamide in the soil inside the bare patch under the canopy of *H .ammodendron* was elevated by 58.02%, while the relative content outside the bare patch dropped to 13.75%. Thus, it can be inferred that the *H. ammodendron* root system continuously secretes oleamide, which gradually accumulates under the canopy of *H. ammodendron*; the content likely gradually decreases with increasing distance, and the higher content of oleamide under the canopy likely inhibits the growth of mosses. Thus, we conclude that oleamide and other amide compounds are the main allelochemicals produced by *H. ammodendron*.

In addition, the soil collected under the moss crusts outside the bare patches contained a large proportion of carbohydrates, including melibiose (21.92%), d-(+)-maltose (20.46%), α,α-trehalose (8.06%) and melezitose (2.32%). These carbohydrates may be produced by *S. caninervis*, which stimulate and enhance the activity of soil microorganisms under the moss crust and thus provide a source of carbon and nitrogen supporting the growth of *S. caninervis*. Such nutrients could facilitate the formation of moss crusts and larger moss patches (Li et al. 2019), as microbial activity is a preliminary process and necessary condition for the formation of biological soil crusts (Maestre et al. 2005; Martínez et al. 2006; Cheng and Zhang 2010). In addition, trehalose can promote plant growth under salt stress (Yuan et al. 2022), and it is suggested that higher concentrations of trehalose can improve the resistance of *S. caninervis* to salt stress.

Finally, phenylpropanoid metabolism was observed in the pathway enrichment analysis, and this pathway is one of the most important metabolisms in plants, contributing to plant development and plant–environment interactions (Dong and Lin 2021). Studies have revealed that drought, salt stress and biotic stresses induce lignin deposition through regulating phenylpropanoid metabolism to enhance stress tolerance in *H. ammodendron* (Nakabayashi and Saito 2015; Li et al. 2022). The litter of *H. ammodendron* is degraded by microorganisms in UC soil, and phenylpropanoid metabolism compounds are dissolved in the soil, where they can gradually form a concentration gradient. However, whether these compounds have an effect on moss growth needs to be verified through further comparisons of moss growth with amide compounds.

Relationship between bare patch formation and soil microbial function

The α-diversity of microorganisms showed that microbial species in UM soil were significantly higher than in UC soil ($P < 0.05$), and the results suggest that biocrusts dominated by mosses can improve the diversity of the subsurface soil microbial community structure by increasing soil stability and fertility. However, based on the PCoA of the relative abundance of microbial communities, KOs and CAZy families showed no significant differences between UC and UM soil, indicating that the formation of the bare patches did not have a significant impact on the structure and function of microbial species. However, changes in microbial abundance inevitably result in corresponding changes in the functional metabolic pathways of the microbial community. KEGG annotations indicated that the relative abundance of enzymes associated with six pathways (Starch and sucrose metabolism, Secretion system, Protein kinases, Peptidoglycan biosynthesis and degradation proteins, Peptidases and inhibitors and Chromosome and associated proteins) were higher in the bare patches, suggesting a high rate of microbial catabolism in the soil inside the bare patches. Li et al. (Li et al. 2020a) found that the abundance of the microbial function associated with the “Starch and sucrose metabolism” pathway was more abundant in soils under moss crusts than in bacterial crusts in the Tengger Desert of China, but the results of the present study showed that the relative abundance of this pathway was higher in soil inside the bare patches. The low abundance of the Starch and sucrose metabolism pathway could result in the accumulation of carbohydrates in rhizosphere soil of the plants (Song et al. 2020). Thus, it can be inferred that the higher abundance of this metabolic pathway could result in an acceleration of carbohydrates decomposition in the bare patches.

CBM5, CBM13, CBM50 and GH18 were relatively abundant in the bare patches, and the first three families belong to the carbohydrate-binding module (CBMs) group in the CAZy database annotation. CBM13 family is the cellulose-binding domain family, which was more abundant in the bare patches of *H. ammodendron* and might be related to plant residue decomposition. Thus, it possible that litter of *H. ammodendron* and residue of *S. caninervis* are degraded quickly to facilitate bare patch formation and plant metabolite accumulation through decomposition by soil microflora. In addition, the development of mosses creates a living environment for insects, which cannot survive once their habitat is destroyed, and it is likely that the other significantly different CAZy families, which were associated with the decomposition of chitin or peptidoglycan, may be related to the decomposition of insect residues (Lizoňová and Horsák 2017; Trekels et al. 2017)

Relationship between microbial communities and soil variables

Species annotation results showed that bacteria were the dominant microbial taxa, and bacterial community was significantly correlated with TN content. Among the top 10 phyla, the four Bacteria phyla Actinobacteria, Proteobacteria, Gemmatimonadetes and Deinococcus-Thermus were significantly different between UM and UC soil, and Actinobacteria and Proteobacteria were the dominant groups. The relative abundance of Actinobacteria was significantly higher in UC soil (59.83%) than in UM soil (56.46%). Actinobacteria can mineralize nitrogen and carbon in soil and decompose organic matter (Li et al. 2010; Kopecky et al. 2011), playing an important role in element cycles and litter decomposition of plants, helping to stabilize soil structure and improving the effectiveness of nutrients and minerals in soil (Solans et al. 2022), which is particularly important for low-fertility soil (Lyra et al. 2021). In this study, correlation analysis results showed that Actinobacteria were significantly negatively correlated with soil TN, and it is inferred that Actinobacteria may prefer oligotrophic environments. The relative abundance of Proteobacteria in UC soil (28.98%) was significantly lower than that in UM soil (33.67%). Reports have shown that the soil bacterial community is rich in Proteobacteria, especially in arid environments and can even account for 70% of the soil bacterial community (Xu et al. 2014; Taketani et al. 2015; Nessner Kavamura et al. 2013). Haichar et al. (Haichar et al. 2008) showed that Proteobacteria (Fierer et al. 2007; Singh et al. 2010) were the main taxa that use plant root secretions and usually respond positively to low-molecular-weight soil metabolites (Goldfarb et al. 2011). Numerous studies have shown that Proteobacteria can promote nutrient absorption and increase plant productivity (Banerjee et al. 2018; Solans et al. 2016), and thus, they had a high relative abundance in soil under the moss crusts. Among the top 30 genera in relative abundance in this study, 8 genera, *Sphingomonas*, *Pseudomonas*, *Bradyrhizobium*, *Methylobacterium*, *Burkholderia*, *Microvirga*, *Mesorhizobium* and *Rhizobium*, all belong to Proteobacteria. Many of them have nitrogen fixation functions, among which *Rhizobium* is the most typical, and it has been shown that most of the bacteria with functions of nitrogen fixation, ammoxidation and denitrification belong to the Proteobacteria (Zhang et al. 2014; Paul 2014), which is inferred to be related to the higher TN content of the soil under the moss crusts.

In this study, correlation analysis showed that Actinobacteria was most likely to be influenced by soil chemical factors, and its abundance was significantly positively correlated with CO_3^{2-}, HCO_3^-, NO_3^--N and pH and negatively correlated with TN; Proteobacteria and Deinococcus-Thermus abundances were both significantly correlated with CO_3^{2-}, TS, NO_3^--N and pH, but Proteobacteria abundance was negatively correlated with these factors. Gemmatimonadetes abundance was only significantly positively correlated with NO_3^--N and pH, while the other six phyla were somewhat correlated with these chemical factors but not significantly.

In addition, correlation analysis showed that Actinobacteria and Gemmatimonadetes abundances were significantly positively correlated with oleamide (Met 1); Actinobacteria, Gemmatimonadetes and Deinococcus-Thermus abundances were significantly positively correlated with (2E,4E)-*N*-(2-methylpropyl) dodeca-2,4-dienamide (Met 5), while Proteobacteria abundance was significantly negatively correlated with Met 5; Actinobacteria and Gemmatimonadetes abundances were significantly positively correlated with elaidic acid (Met 7). Linoleoyl ethanolamide (Met 8) was significantly positively correlated with Deinococcus-Thermus abundance, while it was significantly negatively correlated with Proteobacteria abundance. Overall, both soil metabolites and chemical factors were associated with the microbial community structure of the four bacterial phyla that were significantly different between inside and outside the bare patches, but the association was less than that of TN.

Conclusion

In this study, we provide new insights into the mechanism of bare patch formation under the canopy of *H. ammodendron* and the impact of bare patches on the soil microbial community in the Gurbantunggut Desert, Northern China. Based on soil metabolomics analysis, we found that the amide compounds

secreted by the root system of *H. ammodendron* appear to accumulate at higher concentrations in the soil of bare patches. Among these amide compounds, oleamide is likely to form a concentration gradient around *H. ammodendron* and inhibit the growth of *S. caninervis*. The amide compounds likely have allelopathic effects on the moss.

The formation of the bare patches caused some changes in the chemical properties of the soils inside and outside the patches and also caused changes in the microbial species composition between the two microhabitats, but did not result in significant changes in microbial species and functions. The microbial communities were more strongly associated with soil chemical factors than soil metabolites. Taken together, the results suggest that the amide secondary metabolites produced by *H. ammodendron* inhibit the growth of *S. caninervis* by creating a concentration gradient under its canopy, causing changes in soil chemical factors inside and outside bare patches and thus affecting the abundance of microbial species and relevant metabolic pathways. The differences in microbial communities inside and outside the bare patches are the result of a combination of soil chemical properties and soil metabolites, rather than a direct effect of amide compounds on microbial communities and functions.

Declarations

Funding

This work was supported by the National Natural Science Foundation of China (31860149) and by the National Natural Science Foundation of Xinjiang (2022D01C398).

Competing Interests

The authors declare no confict of interests.

Authors' contribution

The first draft of the manuscript was written by Pei Liu and Eryang Li. Pei Liu prepared the material, collected the data and performed the experiments. Pei Liu, Eryang Li, Yuan Ma and Qinghang Zhang analyzed the data and contributed to the plot making. Jie Lv and Yuan Ma collected soil samples. Jie Lv, Yuan Ma and Pei Liu conceived and designed the experiments. All authors commented on previous versions of the manuscript. All authors have read and approved the final manuscript.

Data Availability

*All sequencing data has been submitted to the NCBI Sequence Read Archive (SRA) (*https://www.ncbi.nlm.nih.gov/sra*) and can be accessed via the following accession numbers: PRJNA897954.*

Acknowledgments

This work was supported by the National Natural Science Foundation of China (31860149) and by the National Natural Science Foundation of Xinjiang (2022D01C398).

References

1. Abdel-Farid IB, Massoud MS, Al-Enazy Y, Abdel Latef AAH, Jahangir M, Gomaa NH (2021) Allelopathic potential of haloxylon persicum against wheat and black mustard with special reference to Its phytochemical composition and antioxidant activity. Agronomy 11:244. https://doi.org/10.3390/agronomy11020244
2. Albuquerque MB, Santos RC, Lima LM, Melo Filho PdA, Nogueira RJMC, Câmara CAG et al (2011) Allelopathy, an alternative tool to improve cropping systems. A review. Agronomy for Sustainable Development 31:379-395. https://doi.org/10.1051/agro/2010031
3. Aramaki T, Blanc-Mathieu R, Endo H, Ohkubo K, Kanehisa M, Goto S et al (2019) KofamKOALA: KEGG Ortholog assignment based on profile HMM and adaptive score threshold. Bioinformatics 36:2251-2252. https://doi.org/10.1093/bioinformatics/btz859
4. Asaduzzaman M, Pratley JE, An M, Luckett DJ, Lemerle D (2015) Metabolomics differentiation of canola genotypes: toward an understanding of canola allelochemicals. Frontiers in Plant Science 5:765. https://doi.org/10.3389/fpls.2014.00765
5. Banerjee S, Schlaeppi K, van der Heijden MGA (2018) Keystone taxa as drivers of microbiome structure and functioning. Nature Reviews Microbiology 16:567-576. https://doi.org/10.1038/s41579-018-0024-1
6. Bao S (2000) Soil and agricultural chemistry analysis, 1st edn. China Agriculture Press, Beijing
7. Bird JA, Herman DJ, Firestone MK (2011) Rhizosphere priming of soil organic matter by bacterial groups in a grassland soil. Soil Biology and Biochemistry 43:718-725. https://doi.org/10.1016/j.soilbio.2010.08.010
8. Bolger AM, Lohse M, Usadel B (2014) Trimmomatic: a flexible trimmer for Illumina sequence data. Bioinformatics 30:2114-2120. https://doi.org/10.1093/bioinformatics/btu170
9. Chen B (2013) Molecular identification and condition culture of cyanobacteria(*Synechococcus*) LZ1. Ocean University of China, Qingdao
10. Chen C, Zhang L, Hu W (1983) The basic characteristics of plant communities, flora and their distribution in the sandy distrct of gurbantungut. Acta Phytoecologica et Geobotanica Sinica 7:89-99

11. Cheng J, Zhang Y (2010) Environmental factors affecting soil bio-crust distribution. Chinese Journal of Ecology 29:133-141. https://doi.org/10.13292/j.1000-4890.2010.0056
12. Cheng N, Peng Y, Kong Y, Li J, Sun C (2018) Combined effects of biochar addition and nitrogen fertilizer reduction on the rhizosphere metabolomics of maize (Zea mays L.) seedlings. Plant and Soil 433:19-35. https://doi.org/10.1007/s11104-018-3811-6
13. Ding J, Eldridge DJ (2021) The fertile island effect varies with aridity and plant patch type across an extensive continental gradient. Plant and Soil 459:173-183. https://doi.org/10.1007/s11104-020-04731-w
14. Dong N, Lin H (2021) Contribution of phenylpropanoid metabolism to plant development and plant-environment interactions. J Integr Plant Biol 63:180-209. https://doi.org/10.1111/jipb.13054
15. Dong W, Xu C, Li D, Jin X, Li R, Lu Q et al (2016) Comparative analysis of the complete chloroplast genome sequences in psammophytic Haloxylon species (Amaranthaceae). PeerJ 4:e2699. https://doi.org/10.7717/peerj.2699
16. Dong Y, Feng L, Wang B, Guo M, Fan X (2018) Allelopathy of aqueous extract of cattail on Microcystis aeruginosa. Chinese Journal of Ecology 37:498-505. https://doi.org/10.13292/j.1000-4890.201802.001
17. Duke, Dayan, Romagni, Rimando (2000) Natural products as sources of herbicides: current status and future trends. Weed Research 40:99-111. https://doi.org/10.1046/j.1365-3180.2000.00161.x
18. Eldridge DJ, Bowker MA, Maestre FT, Roger E, Reynolds JF, Whitford WG (2011) Impacts of shrub encroachment on ecosystem structure and functioning: towards a global synthesis. Ecol Lett 14:709-722. https://doi.org/10.1111/j.1461-0248.2011.01630.x
19. Ewels P, Magnusson M, Lundin S, Käller M (2016) MultiQC: summarize analysis results for multiple tools and samples in a single report. Bioinformatics 32:3047-3048. https://doi.org/10.1093/bioinformatics/btw354
20. Fierer N, Bradford MA, Jackson RB (2007) Toward an ecological classification of soil bacteria. Ecology 88:1354-1364. https://doi.org/https://doi.org/10.1890/05-1839
21. Friedjung AY, Choudhary SP, Dudai N, Rachmilevitch S (2013) Physiological conjunction of allelochemicals and desert plants. PLoS One 8:e81580. https://doi.org/10.1371/journal.pone.0081580
22. Fu L, Niu B, Zhu Z, Wu S, Li W (2012) CD-HIT: accelerated for clustering the next-generation sequencing data. Bioinformatics 28:3150-3152. https://doi.org/10.1093/bioinformatics/bts565
23. Glime JM (2006) Bryophyte ecologyedn. Michigan Technological University, Michigan
24. Goldfarb K, Karaoz U, Hanson C, Santee C, Bradford M, Treseder K et al (2011) Differential growth responses of soil bacterial taxa to carbon substrates of varying chemical recalcitrance. Frontiers in Microbiology 2. https://doi.org/10.3389/fmicb.2011.00094
25. Haichar FeZ, Marol C, Berge O, Rangel-Castro JI, Prosser JI, Balesdent J et al (2008) Plant host habitat and root exudates shape soil bacterial community structure. The ISME Journal 2:1221-1230. https://doi.org/10.1038/ismej.2008.80
26. Ji X, Zhang Y, Tao Z, Zhou X, Zhang J (2013) Size characteristics of the moss crust patches and its relationship to the environmental factors in the gurbantunggut desert. Journal of Desert Research 33:1803-1809. https://doi.org/10.7522/j.issn.1000-694X.2013.00268
27. Johnson D, Vandenkoornhuyse PJ, Leake JR, Gilbert L, Booth RE, Grime JP et al (2004) Plant communities affect arbuscular mycorrhizal fungal diversity and community composition in grassland microcosms. New Phytologist 161:503-515. https://doi.org/10.1046/j.1469-8137.2003.00938.x
28. Jones DL, Willett VB (2006) Experimental evaluation of methods to quantify dissolved organic nitrogen (DON) and dissolved organic carbon (DOC) in soil. Soil Biology and Biochemistry 38:991-999. https://doi.org/10.1016/j.soilbio.2005.08.012
29. Kachurina OM, Zhang H, Raun WR, Krenzer EG (2000) Simultaneous determination of soil aluminum, ammonium- and nitrate-nitrogen using 1 M potassium chloride extraction. Communications in Soil Science and Plant Analysis 31:893-903. https://doi.org/10.1080/00103620009370485
30. Kopecky J, Kyselkova M, Omelka M, Cermak L, Novotna J, Grundmann GL et al (2011) Actinobacterial community dominated by a distinct clade in acidic soil of a waterlogged deciduous forest. FEMS Microbiology Ecology 78:386-394. https://doi.org/10.1111/j.1574-6941.2011.01173.x
31. Lambers H, Chapin FS, Pons TL (2008) Plant physiological escologyedn. Springer, New York
32. Latif S, Chiapusio G, Weston LA (2017) Allelopathy and the role of allelochemicals in plant defence. Academic Press 82:19-54. https://doi.org/10.1016/bs.abr.2016.12.001
33. Li D, Liu C, Luo R, Sadakane K, Lam T (2015) MEGAHIT: an ultra-fast single-node solution for large and complex metagenomics assembly via succinct de Bruijn graph. Bioinformatics 31:1674-1676. https://doi.org/10.1093/bioinformatics/btv033
34. Li J-Y, Jin X-Y, Zhang X-C, Chen L, Liu J-L, Zhang H-M et al (2020a) Comparative metagenomics of two distinct biological soil crusts in the Tengger Desert, China. Soil Biology and Biochemistry 140:107637. https://doi.org/10.1016/j.soilbio.2019.107637
35. Li W, Liu Z, Feng H, Yang J, Li C (2022) Characterization of the Gene Expression Profile Response to Drought Stress in Populus ussuriensis Using PacBio SMRT and Illumina Sequencing. Int J Mol Sci 23. https://doi.org/10.3390/ijms23073840
36. Li X, She Y, Sun B, Song H, Zhu Y, Lv Y et al (2010) Purification and characterization of a cellulase-free, thermostable xylanase from Streptomyces rameus L2001 and its biobleaching effect on wheat straw pulp. Biochemical Engineering Journal 52:71-78. https://doi.org/10.1016/j.bej.2010.07.006
37. Li Y, Xu L, Letuma P, Lin W (2020b) Metabolite profiling of rhizosphere soil of different allelopathic potential rice accessions. BMC Plant Biology 20:265. https://doi.org/10.1186/s12870-020-02465-6
38. Li Y, Zhou X, Zhang Y (2019) Moss patch size and microhabitats influence stoichiometry of moss crusts in a temperate desert, Central Asia. Plant and Soil 443:55-72. https://doi.org/10.1007/s11104-019-04191-x

39. Liu B (2010) Analysis of the degenerated mechanism of haloxylon ammodendron populations in Gurbantunggust Desert. Shihezi University, Shihezi
40. Liu W, Ding J, Zhou J, Lin Z, Tang L (2016) Ultrastructural responses of syntrichia caninervis to a gradient of NaCl stress. Acta Ecologica Sinica 36:3556-3563. https://doi.org/10.5846/stxb201410122011
41. Lizoňová Z, Horsák M (2017) Contrasting diversity of testate amoebae communities in Sphagnum and brown-moss dominated patches in relation to shell counts. Eur J Protistol 58:135-142. https://doi.org/10.1016/j.ejop.2017.02.002
42. Lombard V, Golaconda Ramulu H, Drula E, Coutinho PM, Henrissat B (2013) The carbohydrate-active enzymes database (CAZy) in 2013. Nucleic Acids Research 42:D490-D495. https://doi.org/10.1093/nar/gkt1178
43. Lyra M, Taketani RG, Freitas ADS, Silva C, Mergulhao A, Silva M et al (2021) Structure and diversity of bacterial community in semiarid soils cultivated with prickly-pear cactus (Opuntia ficus-indica (L.) Mill.). An Acad Bras Cienc 93:e20190183. https://doi.org/10.1590/0001-3765202120190183
44. Maestre FT, Escudero A, Martinez I, Guerrero C, Rubio A (2005) Does spatial pattern matter to ecosystem functioning? Insights from biological soil crusts. Functional Ecology 19:566-573. https://doi.org/10.1111/j.1365-2435.2005.01000.x
45. Martínez I, Escudero A, Maestre FT, de la Cruz A, Guerrero C, Rubio A (2006) Small-scale patterns of abundance of mosses and lichens forming biological soil crusts in two semi-arid gypsum environments. Australian Journal of Botany 54:339-348. https://doi.org/10.1071/BT05078
46. Michel P, Burritt DJ, Lee WG (2011a) Bryophytes display allelopathic interactions with tree species in native forest ecosystems. Oikos 120:1272-1280. https://doi.org/10.1111/j.1600-0706.2010.19148.x
47. Michel P, Overton JM, Mason NWH, Hurst JM, Lee WG (2011b) Species–environment relationships of mosses in New Zealand indigenous forest and shrubland ecosystems. Plant Ecology 212:353-367. https://doi.org/10.1007/s11258-010-9827-5
48. Mizutani J (1999) Plant ecochemicals in allelopathy. In: Narwal SS (ed) Basic and applied aspects. Science Publishers Inc, New Hampshire, pp 27–46
49. Nakabayashi R, Saito K (2015) Integrated metabolomics for abiotic stress responses in plants. Curr Opin Plant Biol 24:10-16. https://doi.org/10.1016/j.pbi.2015.01.003
50. Narwal SS (2000) Allelopathy in weed management In: Narwal SS (ed) Basic and applied aspects. Science Publishers Inc, Enfield, pp 203–254
51. Nessner Kavamura V, Taketani RG, Lanconi MD, Andreote FD, Mendes R, Soares de Melo I (2013) Water regime influences bulk soil and Rhizosphere of Cereus jamacaru bacterial communities in the Brazilian Caatinga biome. PLoS One 8:e73606. https://doi.org/10.1371/journal.pone.0073606
52. Olofsdotter M, Jensen LB, Courtois B (2002) Improving crop competitive ability using allelopathy — an example from rice. Plant Breeding 121:1-9. https://doi.org/10.1046/j.1439-0523.2002.00662.x
53. Patro R, Duggal G, Love MI, Irizarry RA, Kingsford C (2017) Salmon provides fast and bias-aware quantification of transcript expression. Nature Methods 14:417-419. https://doi.org/10.1038/nmeth.4197
54. Paul EA (2014) Soil microbiology, ecology and biochemistry, 4th edn. Academic press, UK
55. Pétriacq P, Williams A, Cotton A, McFarlane AE, Rolfe SA, Ton J (2017) Metabolite profiling of non-sterile rhizosphere soil. The Plant Journal 92:147-162. https://doi.org/10.1111/tpj.13639
56. Qian Y, Zhang L, Wu Z (2002) Damage and recovery of the Gurbantunggut Desert vegetation following engineering activities. Science in China Series D: Earth Sciences 45:78-86. https://doi.org/10.1007/BF02878392
57. Rice EL (1984) Allelopathy, 2nd edn. Academic Press, Orlando
58. Rydin H (2008) Population and community ecology of bryophytes. In: Shaw AJ, Goffinet B (ed) Bryophyte biology, 2rd edn. Cambridge University Press, Cambridge, pp 393-444
59. Seemann T (2014) Prokka: rapid prokaryotic genome annotation. Bioinformatics 30:2068-2069. https://doi.org/10.1093/bioinformatics/btu153
60. Shao J, He Y, Li F, Zhang H, Chen A, Luo S et al (2016) Growth inhibition and possible mechanism of oleamide against the toxin-producing cyanobacterium Microcystis aeruginosa NIES-843. Ecotoxicology 25:225-233. https://doi.org/10.1007/s10646-015-1582-x
61. Silva AT, Gao B, Fisher KM, Mishler BD, Ekwealor JTB, Stark LR et al (2021) To dry perchance to live: Insights from the genome of the desiccation-tolerant biocrust moss Syntrichia caninervis. The Plant Journal 105:1339-1356. https://doi.org/10.1111/tpj.15116
62. Singh BK, Bardgett RD, Smith P, Reay DS (2010) Microorganisms and climate change: terrestrial feedbacks and mitigation options. Nature Reviews Microbiology 8:779-790. https://doi.org/10.1038/nrmicro2439
63. Solans M, Pelliza YI, Tadey M (2022) Inoculation with native actinobacteria may improve desert plant growth and survival with potential use for restoration practices. Microbial Ecology 83:380-392. https://doi.org/10.1007/s00248-021-01753-4
64. Solans M, Vobis G, Jozsa L, Wall LG (2016) Synergy of actinomycete co-inoculation. In: Subramaniam G, et al (ed). Springer Singapore, Singapore, pp 161-177
65. Song Y, Li X, Yao S, Yang X, Jiang X (2020) Correlations between soil metabolomics and bacterial community structures in the pepper rhizosphere under plastic greenhouse cultivation. Science of The Total Environment 728:138439. https://doi.org/10.1016/j.scitotenv.2020.138439
66. Sun S, Zhuang L, Li W-h, Zhang G, Xu Z, Zhan D (2010) Relationship between protective enzyme activity of haloxylon ammodendron and edaphon number in the south junggar basin. Arid Zone Research 27:921-926. https://doi.org/10.13866/j.azr.2010.06.015
67. Swenson TL, Jenkins S, Bowen BP, Northen TR (2015) Untargeted soil metabolomics methods for analysis of extractable organic matter. Soil Biology and Biochemistry 80:189-198. https://doi.org/10.1016/j.soilbio.2014.10.007
68. Taketani RG, Kavamura VN, Mendes R, Melo IS (2015) Functional congruence of rhizosphere microbial communities associated to leguminous tree from Brazilian semiarid region. Environmental Microbiology Reports 7:95-101. https://doi.org/10.1111/1758-2229.12187

69. Trekels H, Driesen M, Vanschoenwinkel B (2017) How do patch quality and spatial context affect invertebrate communities in a natural moss microlandscape? Acta Oecologica 85:126-135. https://doi.org/https://doi.org/10.1016/j.actao.2017.10.003
70. Wang J, Zhan J, Wu C, Zhao G (2016) Allelochemicals and its mechanism. Feed Review 04:14-17
71. Wang S, Han X, Qiao Y (2007) Allelopathy of root exudates and their effects on rhizosphere microorganism. Chinese Journal of Soil Science:1219-1226. https://doi.org/10.19336/j.cnki.trtb.2007.06.038
72. Wang X, Zhang Y, Wang Y, Wan J, Xu M (2006) Eco-environment change of biological crusts on longitudinal dune surface in Gurbantunggut Desert. Journal of Desert Research 26:711-716. https://doi.org/10.3321/j.issn:1000-694X.2006.05.007
73. Wang Y, Li X, Wu X, Hong Y, Wang T, Zuo F et al (2021) Divergent effects of biological soil crusts on soil respiration between bare patches and shrub patches under simulated rainfall in a desert ecosystem in Northwest China. Soil and Tillage Research 214:105-185. https://doi.org/10.1016/j.still.2021.105185
74. Want EJ, Masson P, Michopoulos F, Wilson ID, Theodoridis G, Plumb RS et al (2013) Global metabolic profiling of animal and human tissues via UPLC-MS. Nature Protocols 8:17-32. https://doi.org/10.1038/nprot.2012.135
75. Wen B, Mei Z, Zeng C, Liu S (2017) metaX: a flexible and comprehensive software for processing metabolomics data. BMC Bioinformatics 18:183. https://doi.org/10.1186/s12859-017-1579-y
76. White RA, Rivas-Ubach A, Borkum MI, Köberl M, Bilbao A, Colby SM et al (2017) The state of rhizospheric science in the era of multi-omics: A practical guide to omics technologies. Rhizosphere 3:212-221. https://doi.org/10.1016/j.rhisph.2017.05.003
77. Wood DE, Salzberg SL (2014) Kraken: ultrafast metagenomic sequence classification using exact alignments. Genome Biology 15:R46. https://doi.org/10.1186/gb-2014-15-3-r46
78. Wu X, Wu H, Zhong B, Ye J (2016) Experimental study on the inhibition effect of extracts from pistia stratiotes linn. on the growth of Microcystis aeruginosa. Acta Hydrobiologica Sinica 40:547-551. https://doi.org/10.7541/2016.73
79. Wu X, Zheng X, Mu X, Li Y (2021) Differences in allometric relationship of two dominant woody species among various terrains in a Desert Region of Central Asia. Frontiers in Plant Science 12:754887. https://doi.org/10.3389/fpls.2021.754887
80. Xiao L, Lin Y, Xu B, Yu Y, Liu T (2015) Study on allelopathy and identification of allelochemical in rhizosphere soil of polygonatum. Chinese Agricultural Science Bulletin 31:163-167
81. Xu Z, Hansen MA, Hansen LH, Jacquiod S, Sorensen SJ (2014) Bioinformatic approaches reveal metagenomic characterization of soil microbial community. PLoS One 9:e93445. https://doi.org/10.1371/journal.pone.0093445
82. Yin B, Zhang Y, Lou A (2017) Impacts of the removal of shrubs on the physiological and biochemical characteristics of Syntrichia caninervis Mitt: in a temperate desert. Scientific Reports 7:45268. https://doi.org/10.1038/srep45268
83. Yin BF, Zhang YM (2016) Physiological regulation of Syntrichia caninervis Mitt. in different microhabitats during periods of snow in the Gurbantünggüt Desert, northwestern China. J Plant Physiol 194:13-22. https://doi.org/10.1016/j.jplph.2016.01.015
84. Yu H, Shen G, Gao X (2013) Determination of tobacco root exudates by GC-MS. Acta Tabacaria Sinica 19:64-72. https://doi.org/10.3969/j.issn.1004-5708.2013.04.011
85. Yuan G, Sun D, An G, Li W, Si W, Liu J et al (2022) Transcriptomic and metabolomic analysis of the effects of exogenous trehalose on salt tolerance in Watermelon (Citrullus lanatus). Cells 11:2338. https://doi.org/10.3390/cells11152338
86. Zak DR, Holmes WE, White DC, Peacock AD, Tilman D (2003) Plant diversity, soil microbial communities, and ecosystem function: are there any links? Ecology 84:2042-2050. https://doi.org/10.1890/02-0433
87. Zak JC, Willig MR, Moorhead DL, Wildman HG (1994) Functional diversity of microbial communities: A quantitative approach. Soil Biology and Biochemistry 26:1101-1108. https://doi.org/10.1016/0038-0717(94)90131-7
88. Zhang L, Liu S, Zhou Jx, Huang Q (1998) The affection of engineering action on the vegetation in the gurbantongut desert. Arid Zone Research 15:16-21. https://doi.org/10.13866/j.azr.1998.04.004
89. Zhang R, Zhang D, Bai J, Chen H, Gao Y (2006) Constituents in root secreta of *Haloxylon ammodendron* (c. A. Mey.) bunge seedlings at different ages. Acta Botanica Boreali-Occidentalia Sinica:2150-2154
90. Zhang R, Zhang D, Bai J, Chen H, Gao Y (2007) Study on the extracts methods of the root exudates from the seedling of *Haloxylon ammodendron* (c. A.mey.) bunge. Journal of Arid Land Resources and Environment 153-157. https://doi.org/10.13448/j.cnki.jalre.2007.03.033
91. Zhang Y, Cao C, Peng M, Xu X, Zhang P, Yu Q et al (2014) Diversity of nitrogen-fixing, ammonia-oxidizing, and denitrifying bacteria in biological soil crusts of a revegetation area in Horqin Sandy Land, Northeast China. Ecological Engineering 71:71-79. https://doi.org/10.1016/j.ecoleng.2014.07.032
92. Zhang Y, Chen J, Wang X, Pan H, Gu Z, Pan B (2005) The distribution patterns of biological soil crust in Gurbantunggut Desert. Acta Geographica Sinica 60:53-60. https://doi.org/10.3321/j.issn:0375-5444.2005.01.006
93. Zhang Y, Pan H, Pan B (2004) Distribution characteristics of biological crust on sand dune surface in gurbantunggut desert, Xinjiang. Journal of Soil and Water Conservation 18:61-64. https://doi.org/10.3321/j.issn:1009-2242.2004.04.016
94. Zhang Y, Wu N, Zhang B, Zhang J (2010) Species composition, distribution patterns and ecological functions of biological soil crusts in the Gurbantunggut Desert. Journal of Arid Land 2:180-189. https://doi.org/10.3724/SP.J.1227.2010.00180
95. Zhang Z, Liang A, Dong Z, Zhang Z (2022) Sand provenance in the Gurbantunggut Desert, northern China. CATENA 214:106242. https://doi.org/https://doi.org/10.1016/j.catena.2022.106242

96. Zhang Z, Liu Y, Yuan L, Weber E, van Kleunen M (2020) Effect of allelopathy on plant performance: a meta-analysis. Ecology Letters 24:348-362. https://doi.org/10.1111/ele.13627

Figures

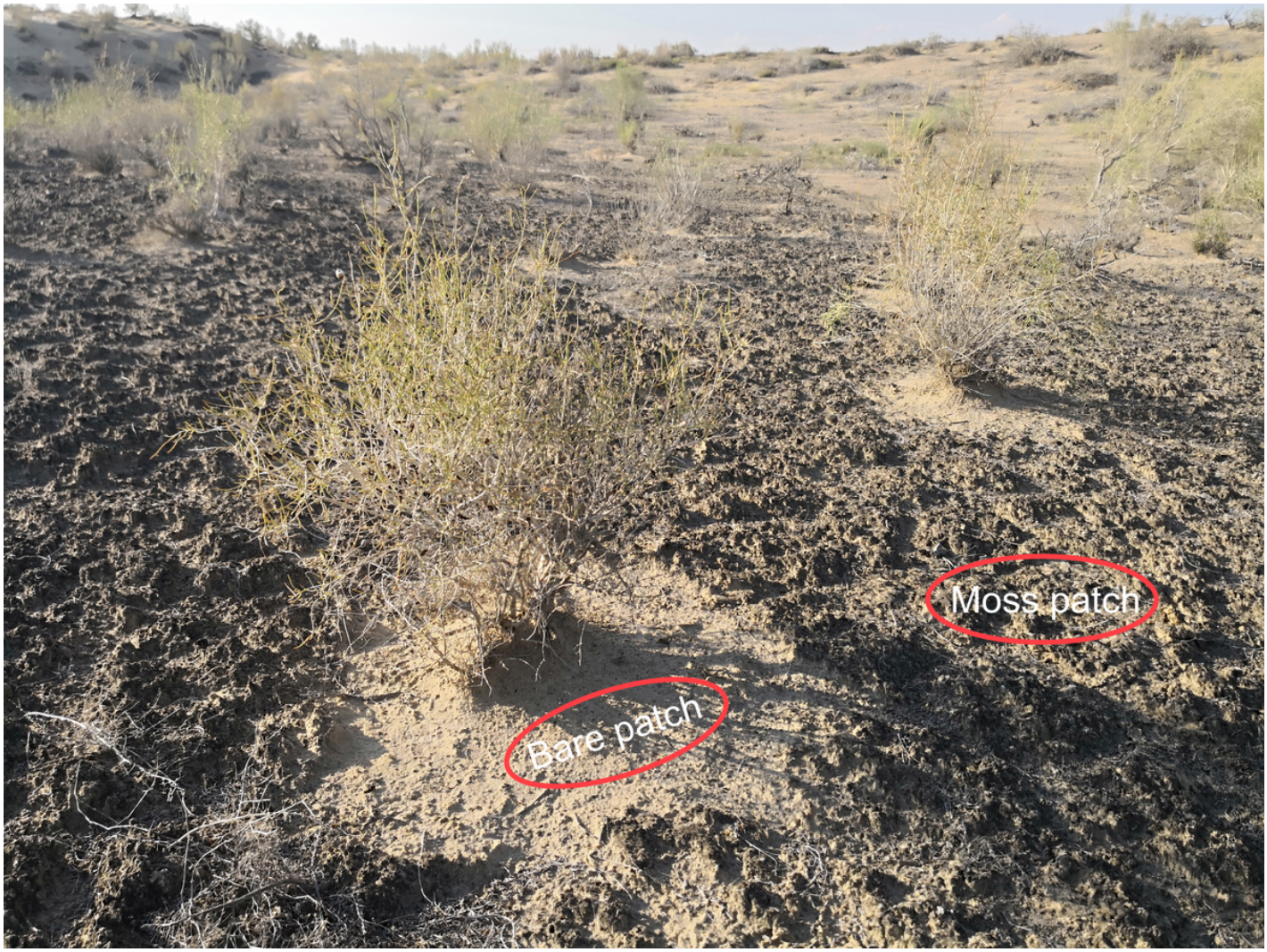

Figure 1

Landscape of the study sites.

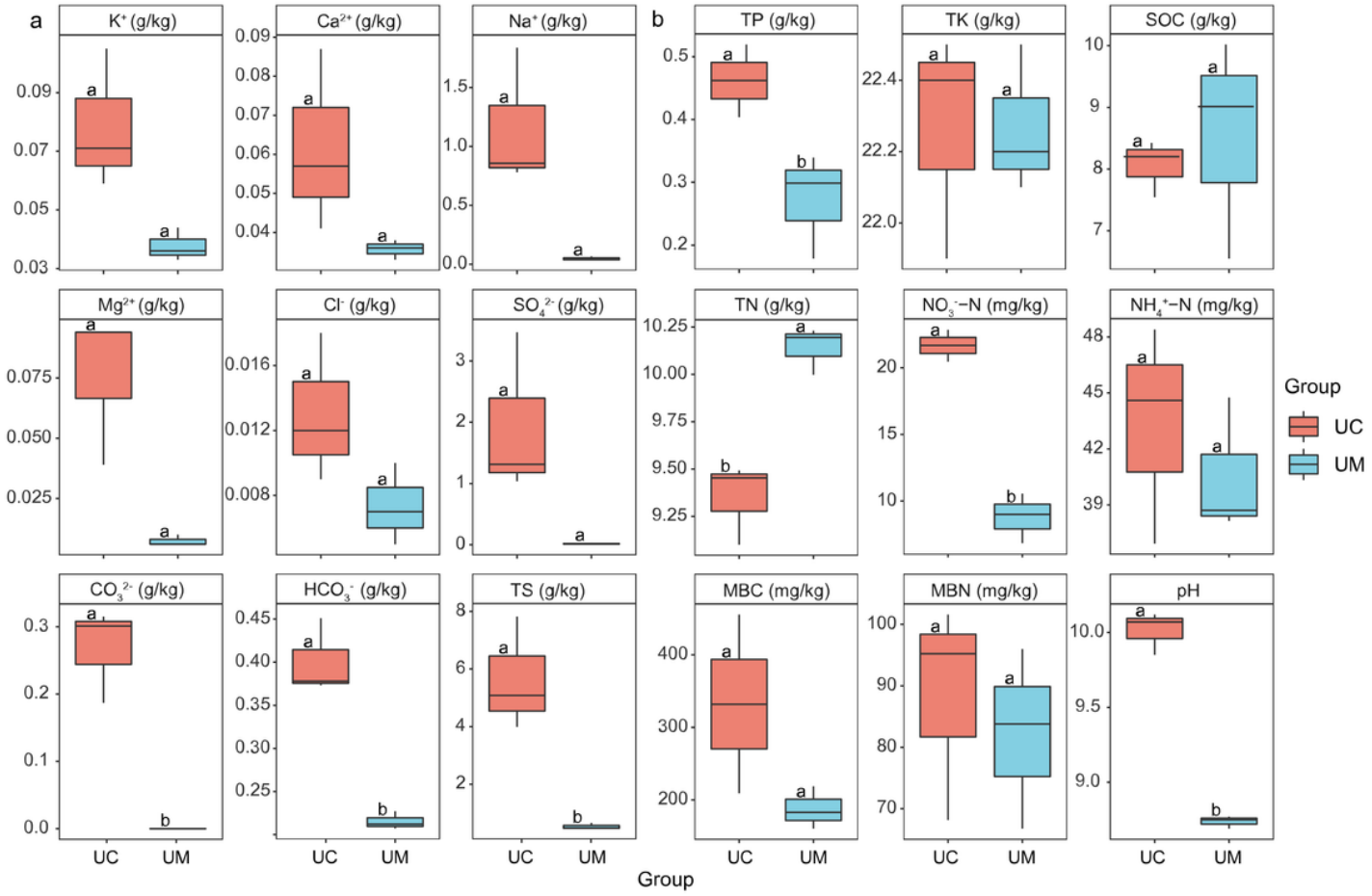

Figure 2

Comparison of soil chemical properties inside and outside of the bare patches

Note: Different letters indicate significant differences ($P < 0.05$), as indicated by a *t*-test; UC, under the *H. ammodendron* canopy or inside the bare patch; UM, under the moss crust or outside the bare patch; TS, total salt; TP, total phosphorus; TK, total potassium; SOC, soil organic carbon; TN, total nitrogen; MBC, microbial biomass carbon; MBN, microbial biomass nitrogen.

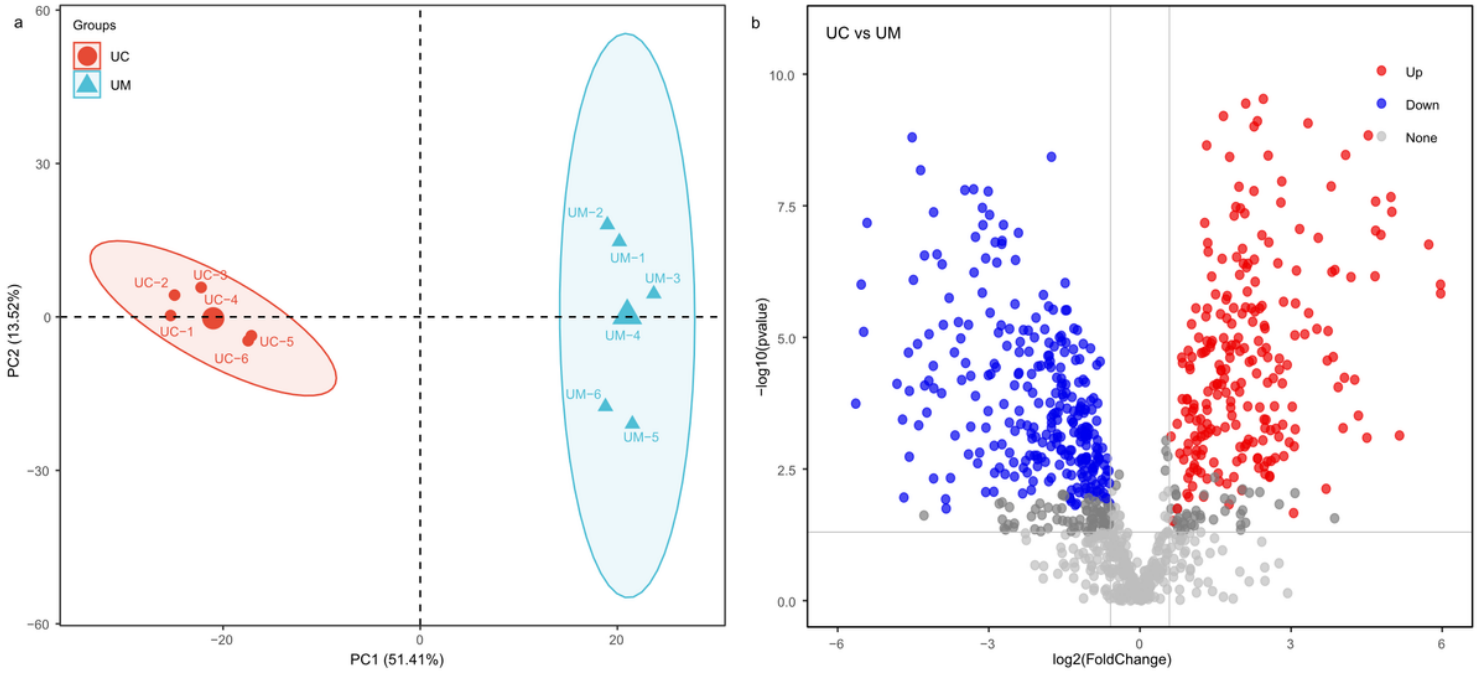

Figure 3

(a) Principal component analysis (PCA) of identified metabolites. (b) Volcano plot of differential metabolites.

Note: In (b), each dot represents a metabolite. “Red” indicates significant up-regulation, and “blue” indicates significant down-regulation. The closer the dot is to the upper left and upper right of the plot, the larger the fold change (FC) of the metabolite and the smaller the *P*-value. The abscissa shows $\log_2$(FC) values; the ordinate shows the -$\log_{10}$(*P*-value) of a *t*-test.

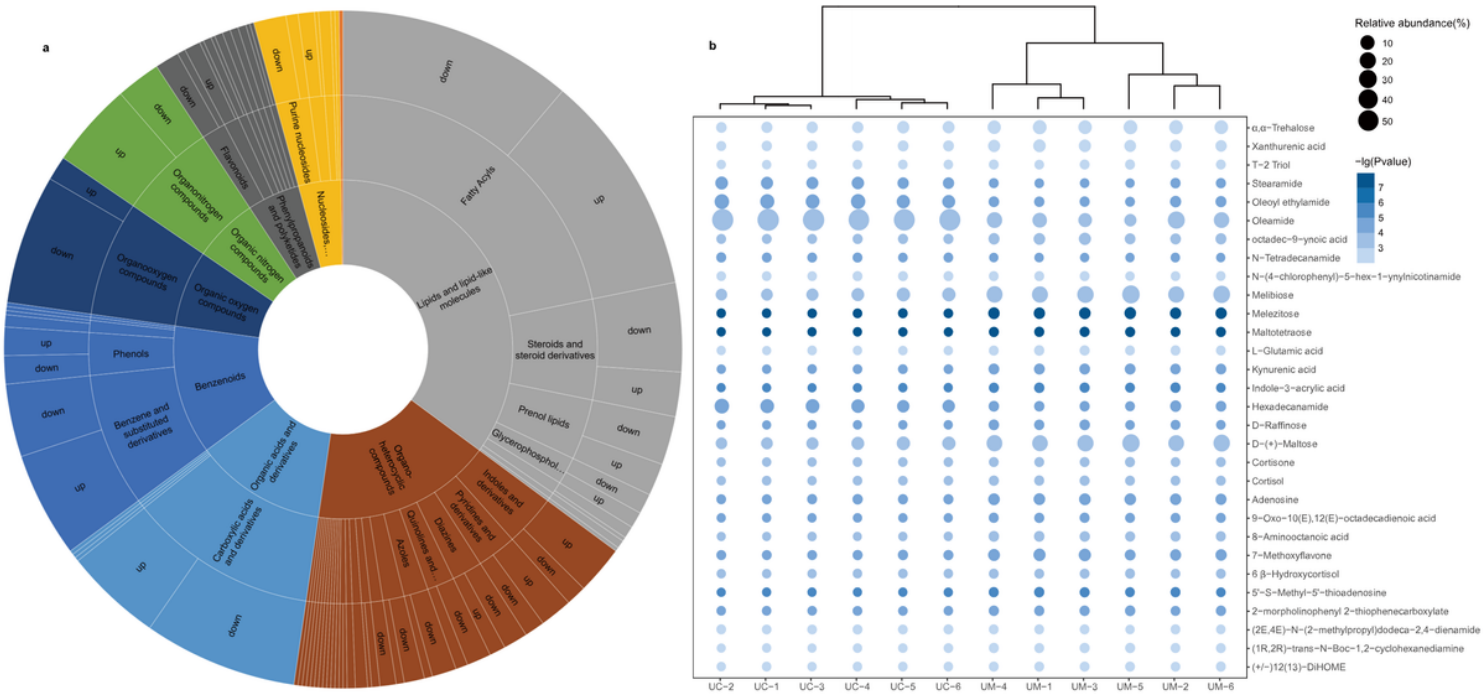

Figure 4

(a) Classification of 518 differential metabolites identified. (b) Cluster bubble chart of the top 30 plant metabolites by abundance.

Note: In (b), the size of the bubble represents the relative abundance, with larger bubbles indicating higher relative abundance; -lg(*P*) values are the negative log-base-10 transformation of the *P*-value obtained using a *t*-test, with darker colors indicating smaller *P*-values.

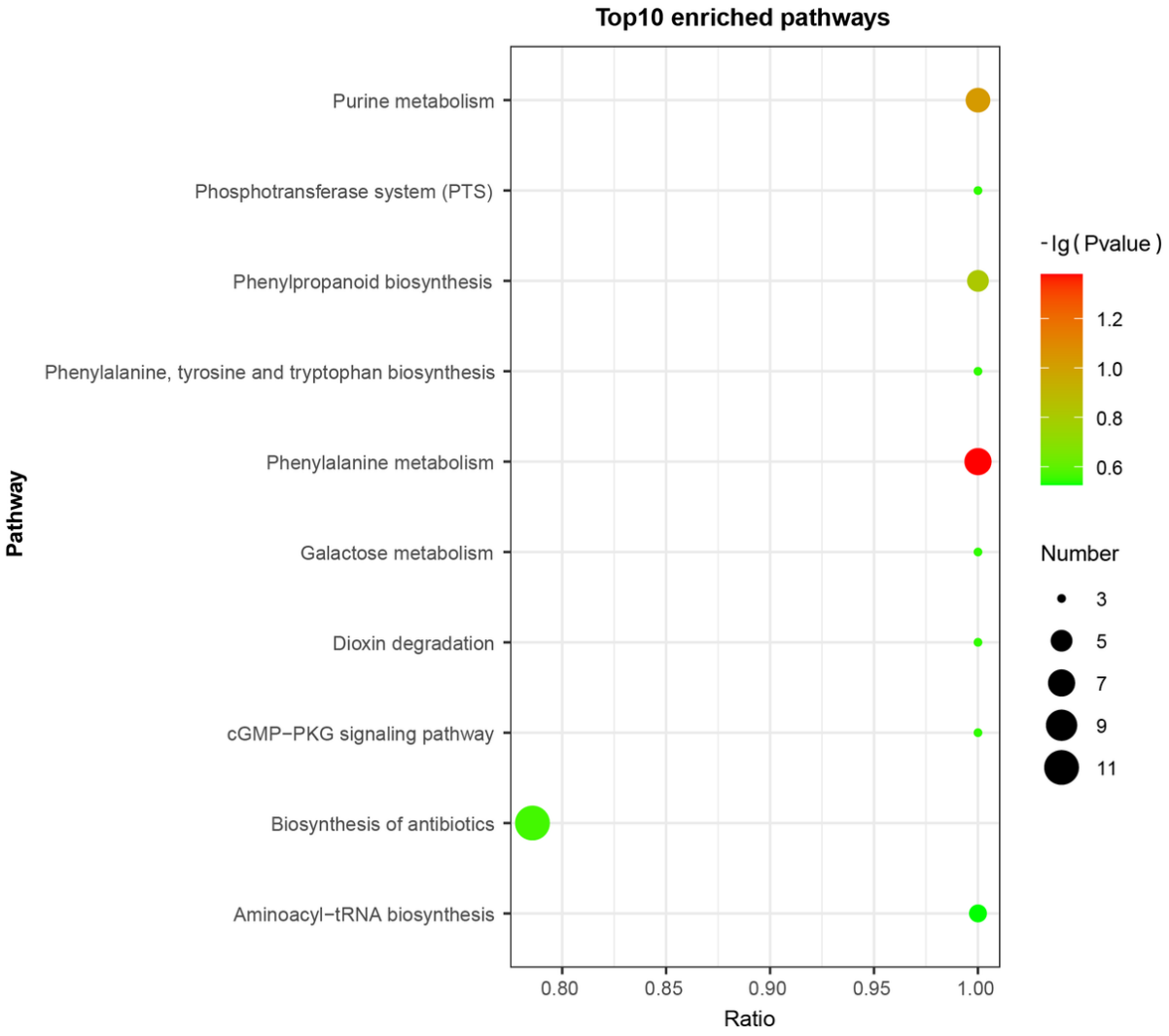

Figure 5

Bubble chart of KEGG enrichment analysis (inside (UC) versus outside (UM) the bare patches)

Note: Ratio = the number of differential metabolites in the corresponding metabolic pathway / the number of total metabolites identified in that pathway

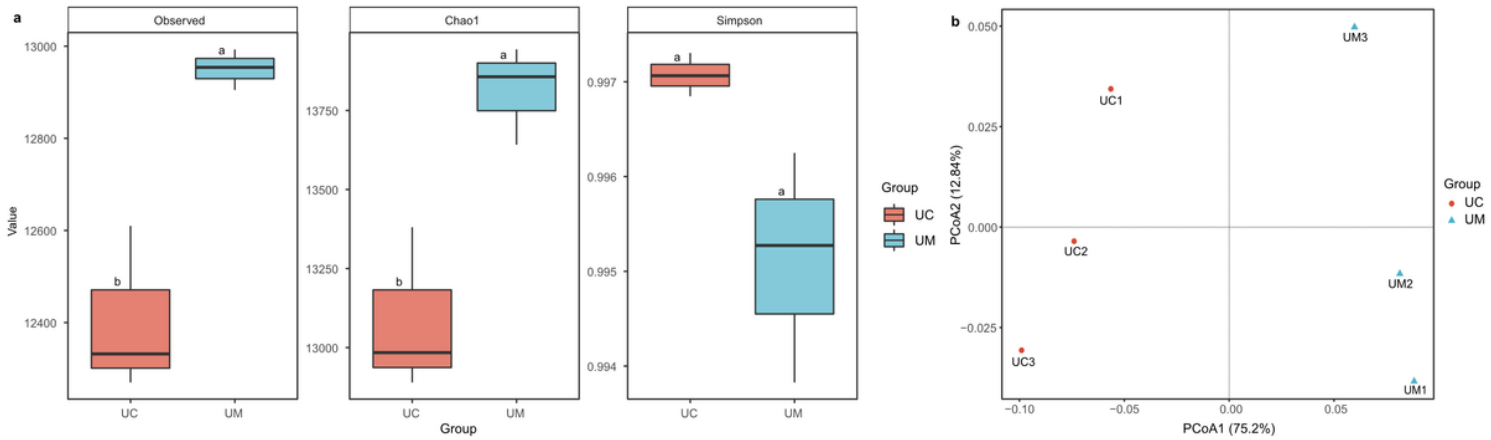

Figure 6

Microbial diversity analysis in soils inside and outside the bare patches. (a) The alpha diversity of microorganisms in soils inside and outside the bare patches. (b) Principal co-ordinate analysis (PCoA) of soil microbial community structure inside and outside the bare patches based on Bray–Curtis distance.

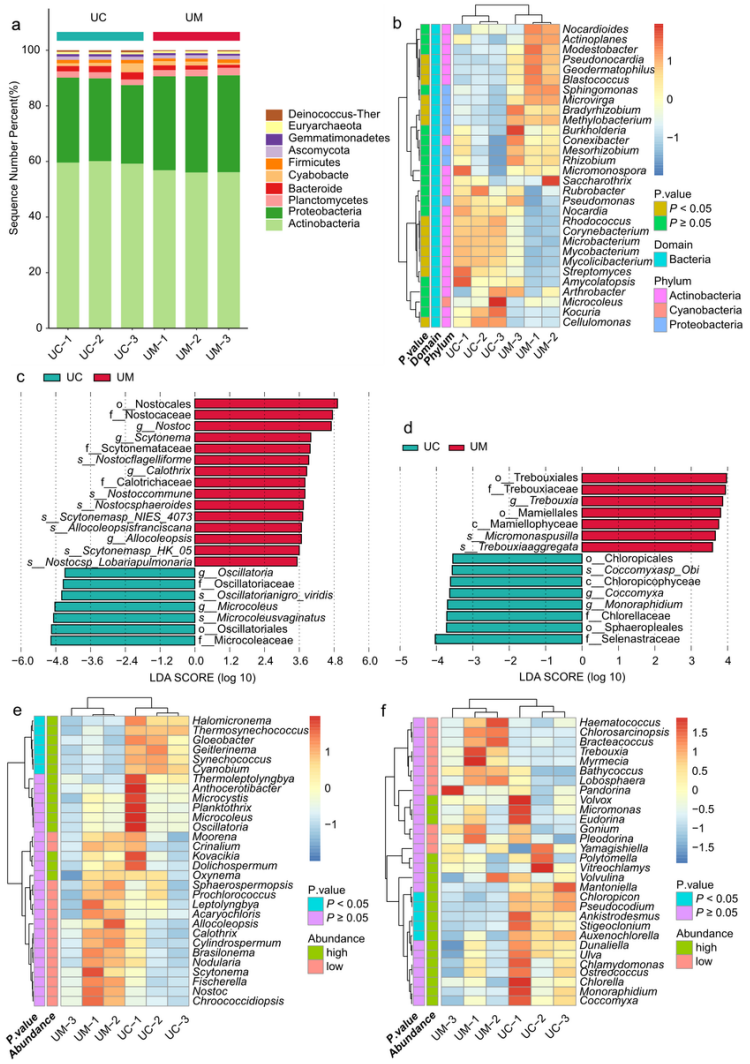

Figure 7

(a) Species relative abundance at the phylum level in soils inside and outside bare patches (Top 10). (b) Heatmap of relative abundances of species at the genus level in soils inside and outside the bare patches (Top 30). (c) Linear discriminant analysis of effect size of Cyanobacteria. d. Linear discriminant analysis of effect size of Chlorophyta. (e) Heatmap of relative abundances of Cyanobacteria in soils inside and outside the bare patches (Top 30). (f) Heatmap of relative abundances of Chlorophyta in soils inside and outside the bare patches (Top 30). For abundance shown in (e) and (f), high means the relative abundance in UC soil was higher than that in UM soil, while low means the relative abundance in UC soil was lower than that in UM soil.

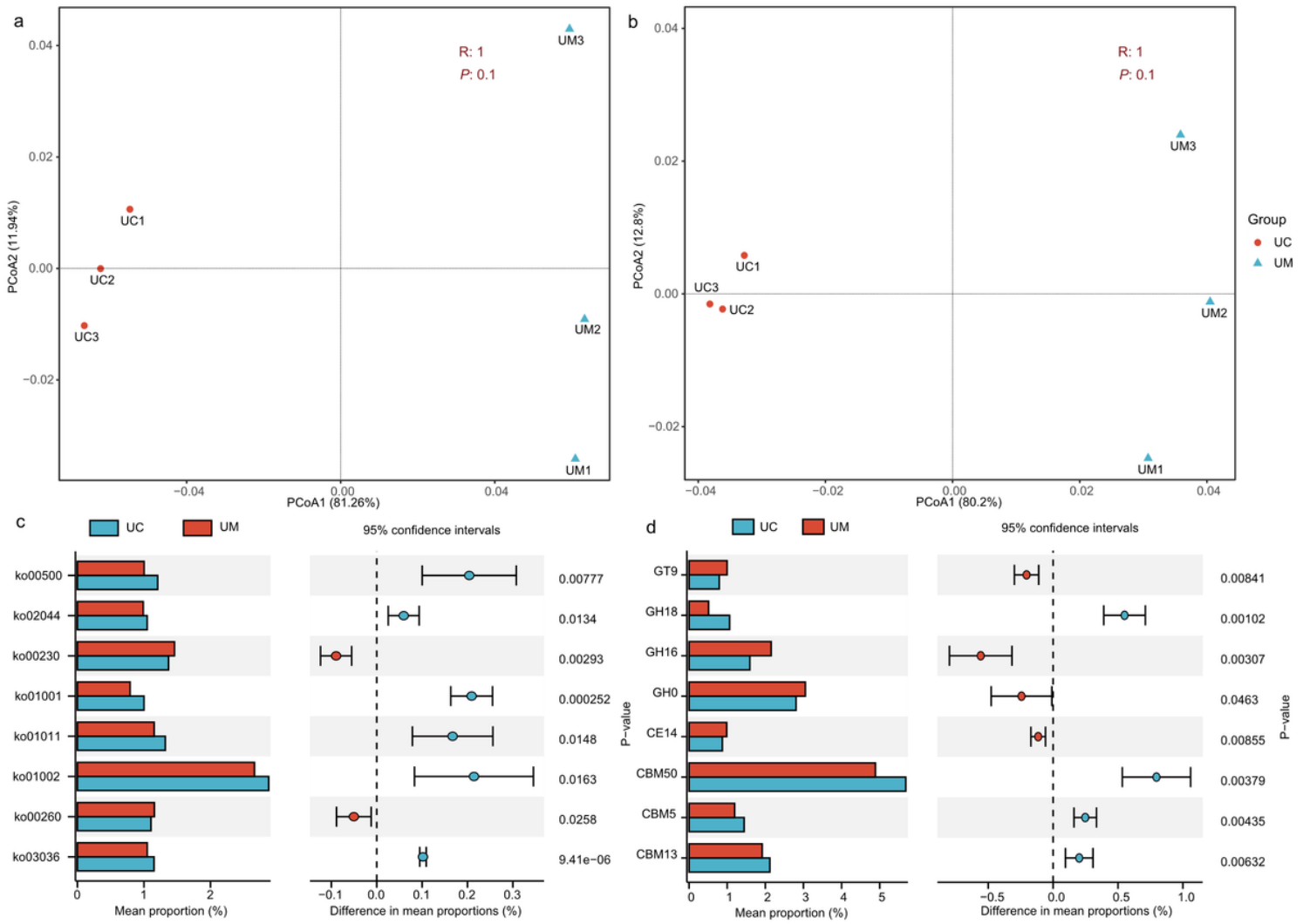

Figure 8

Functional diversity comparison of microbial communities in soils inside and outside the bare patches. (a) Principal coordinate analysis (PCoA) at the KEGG ortholog level. (b) PCoA analysis of CAZy families. (c) and (d) Significant difference analysis at the KEGG ortholog level and in CAZy families (relative abundance > 1%).

Note: In (c) ko00500, Starch and sucrose metabolism; ko02044, Secretion system; ko00230, Purine metabolism; ko01001, Protein kinases; ko01011, Peptidoglycan biosynthesis and degradation proteins; ko01002, Peptidases and inhibitors; ko00260, Glycine, serine and threonine metabolism; ko03036, Chromosome and associated proteins.

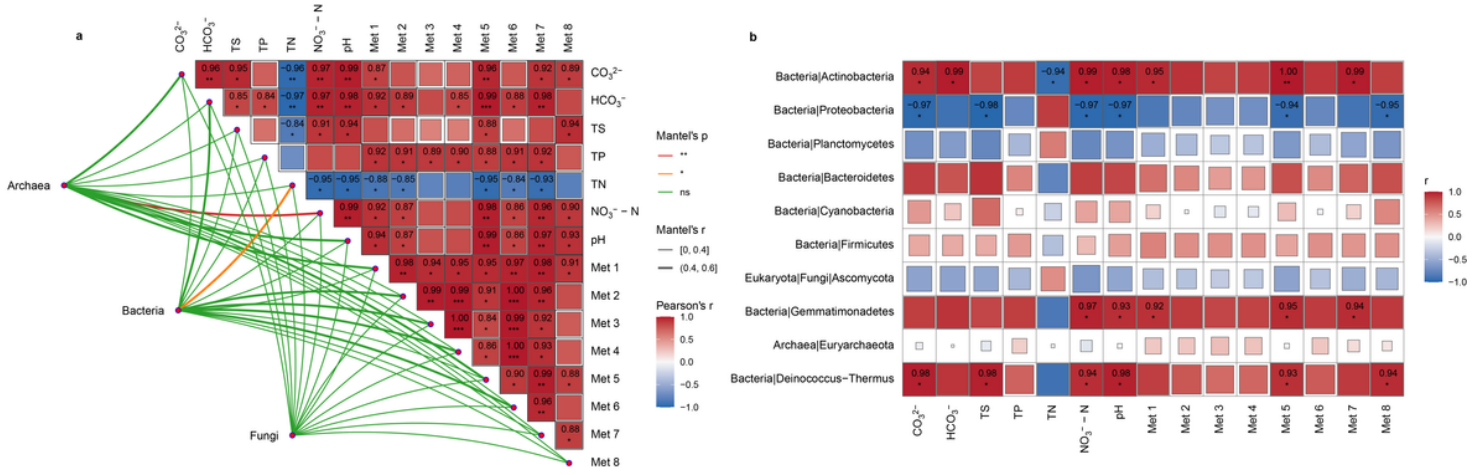

Figure 9

(a) Relationships between soil variables and microbial community structure. (b) Correlation heatmap of microbial communities (phylum level) with soil variables.

Note: Soil variables include soil chemical properties and major metabolites. Met1–8: Met 1, oleamide; Met 2, oleoyl ethylamide; Met 3, hexadecanamide; Met 4, stearamide; Met 5, (2E,4E)-*N*-(2-methylpropyl)dodeca-2,4-dienamide; Met 6, *N*-tetradecanamide; Met 7, elaidic acid; Met 8, linoleoyl ethanolamide. Associations between taxonomic groups and each soil variable were analyzed by Mantel test. Pairwise comparisons of environmental factors are displayed with the color gradient denoting Spearman's correlation coefficients. Relevance is indicated by the size of the square and the depth of the color. *, $P < 0.05$; ** $P < 0.01$; *** $P < 0.001$.

Supplementary Files

This is a list of supplementary files associated with this preprint. Click to download.

- SupplementaryInformation.pdf